Multimode Dynamics in Ring Lasers

ANTONIO PÉREZ-SERRANO

IFISC

I. Introduction

II. Modal Structure of Ring Lasers

III. Multimode Dynamics in Ring Lasers

I. Introduction

I.a. Motivation

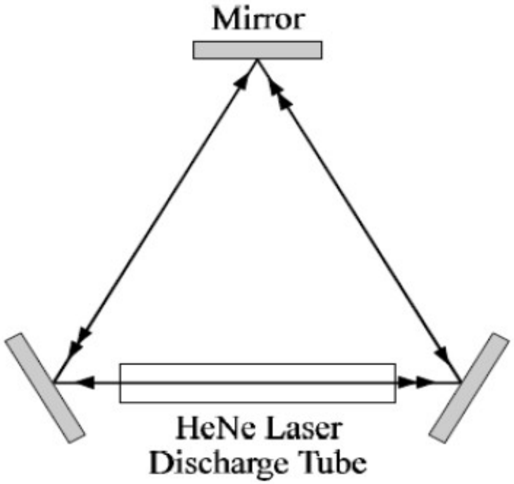

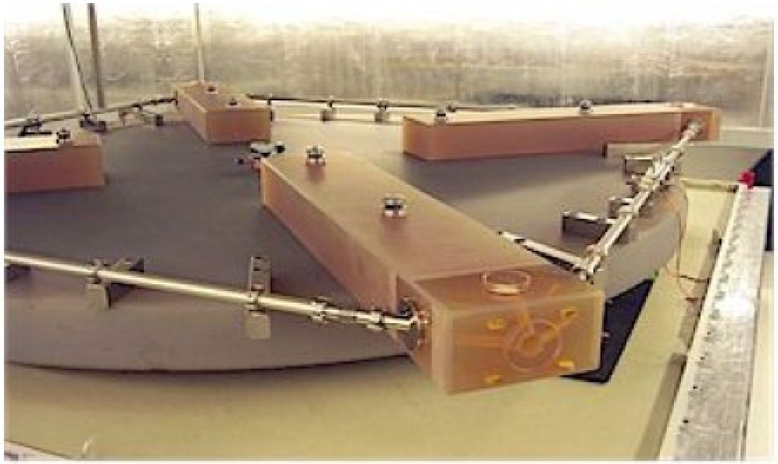

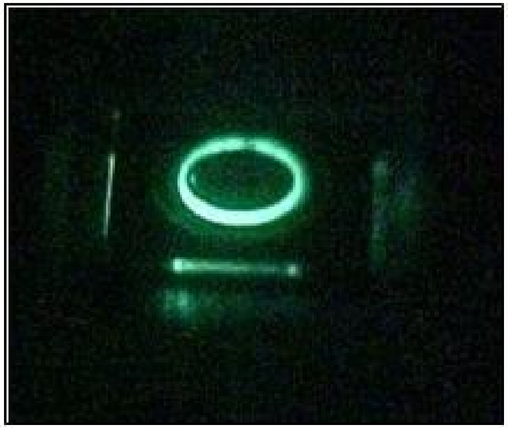

IR picture of a working SRL

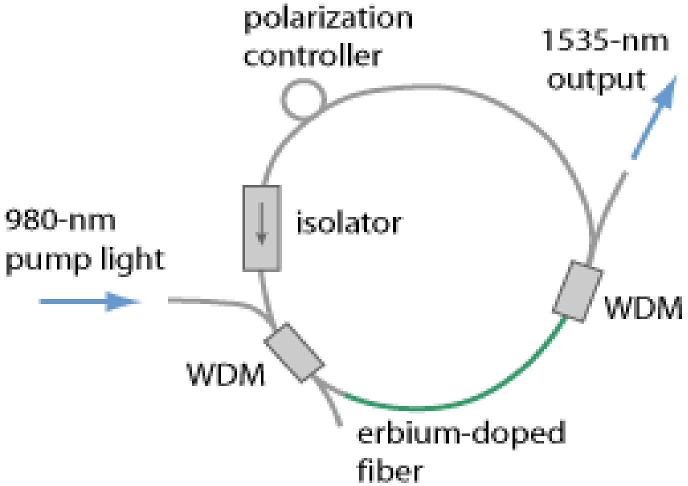

I.a. Motivation

Fabry-Pérot:

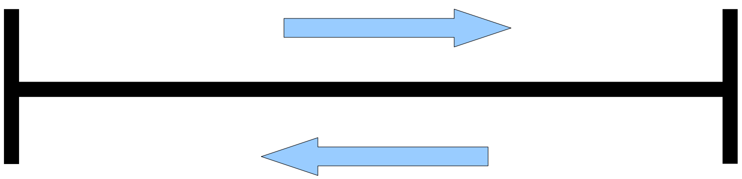

Ring:

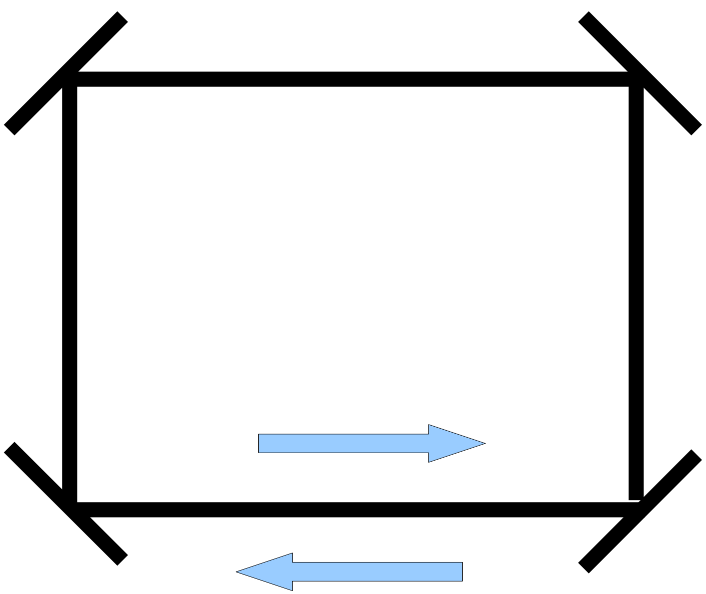

Rich dynamical variety:

Continuous Wave (CW)

Mode-locking

Q-switching

Chaos

+ Dynamical regimes

Alternate Oscillations

Directional Bistability

...

Fiber Ring Laser:

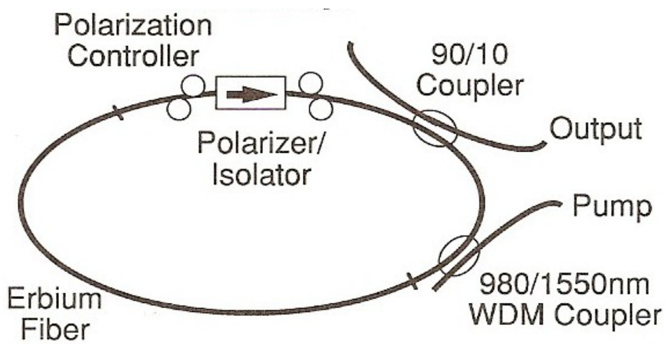

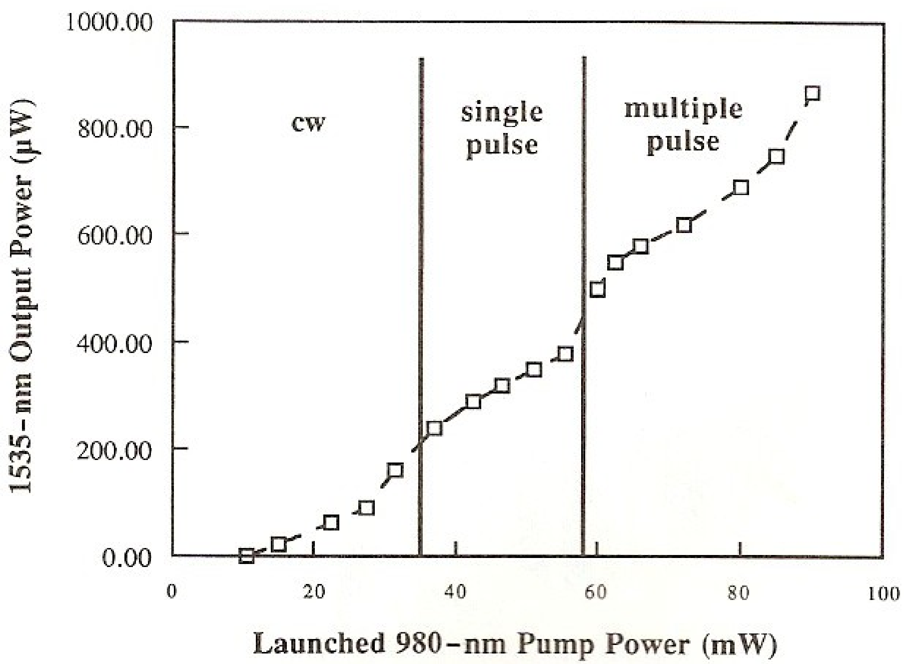

Single pulse

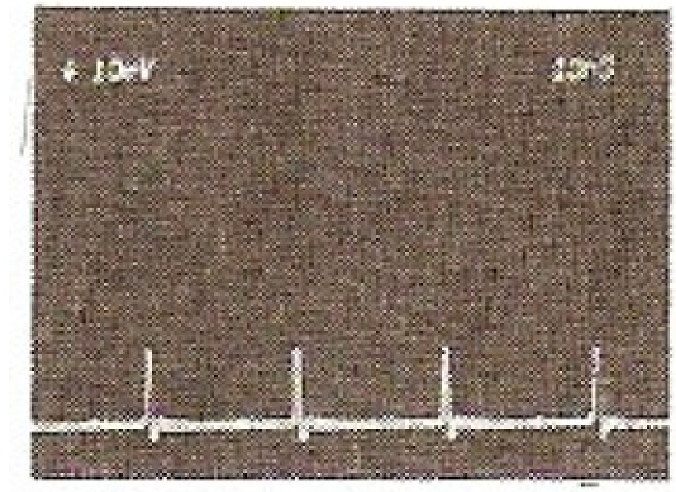

Tamura et al. Opt. Lett. 18, 220 (1993)

Semiconductor Ring Laser:

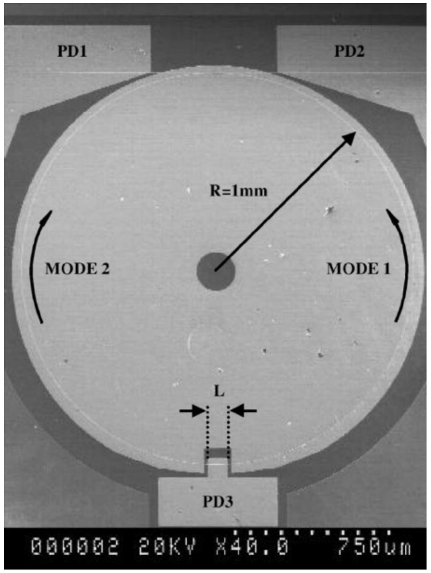

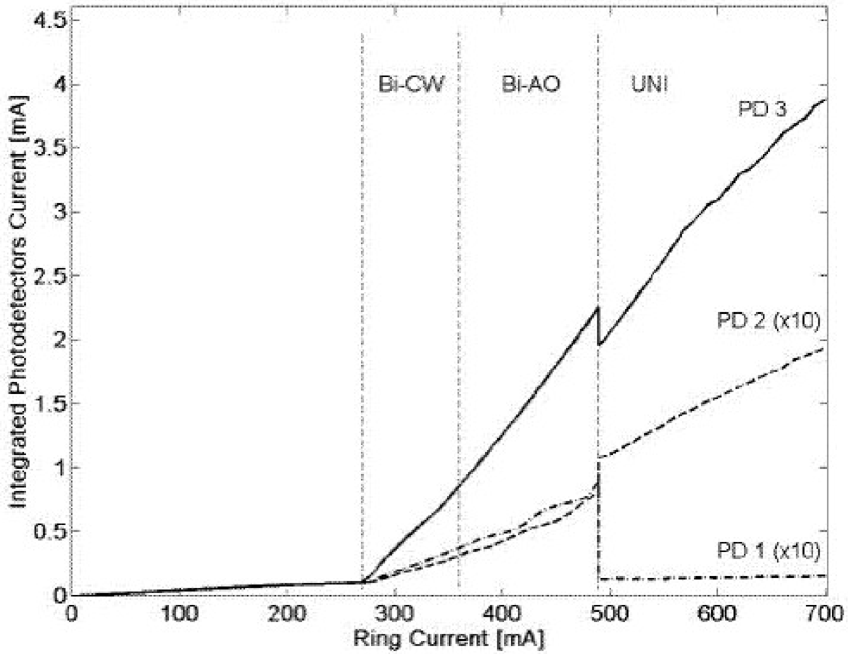

Bi-AO

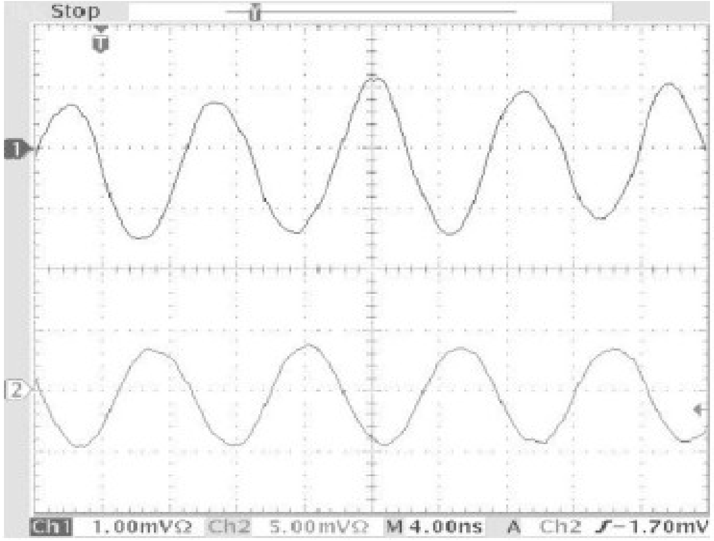

Sorel et al. IEEE JQE 39, 1187 (2003)

I.b. Applications

- Gyroscope (Sagnac Effect)

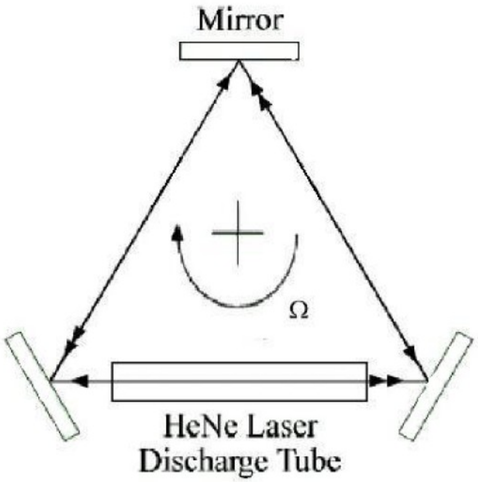

- Optical Memory (Directional Bistability)

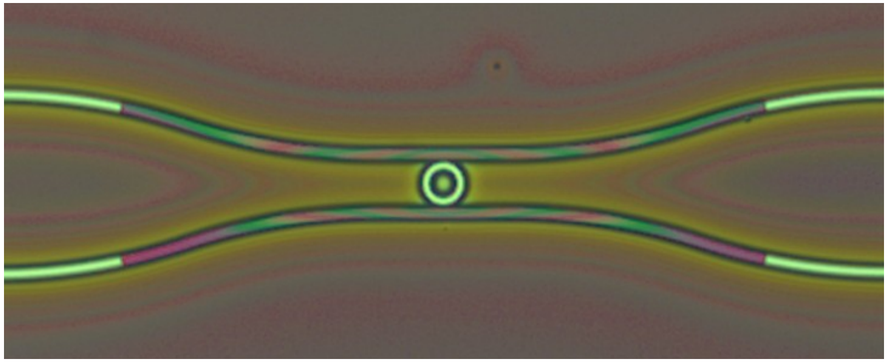

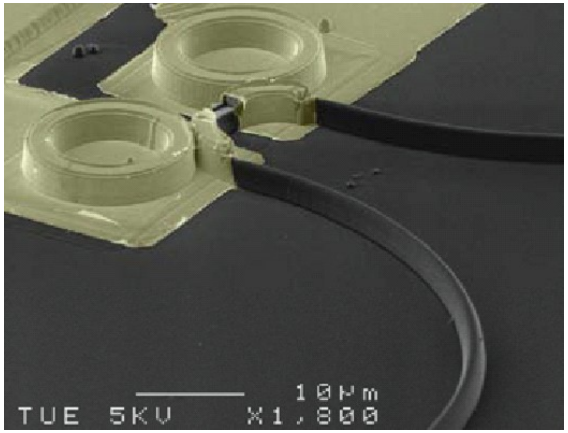

[Hill et al., A fast low-power optical memory based on coupled micro-ring lasers, Nature 2004]

I.c. Methodology

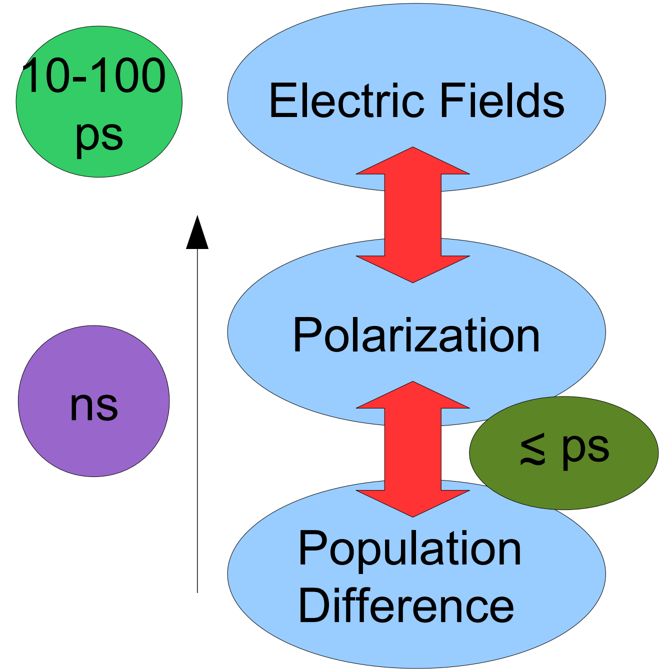

Models:

- Rate Equations Models: ODEs

  Spatial effects (Mean Field Approx.)
  Adiabatic Elimination of the Polarization
  Usually Singlemode
  Low computational cost

Zeghlache et al. PRA **37**, 470 (1988)
Vermuri and Roy, PRA **39**, 4668 (1989)
Sorel et al, IEEE JQE **39**, 1187 (2003)
Roldán and Valcárcel, Europhys. Lett. **43**, 255 (1998)

- Travelling Wave Models: PDEs

  Spatial effects retained
  Singlemode or Multimode
  High computational cost

Fleck, PRB **1**, 84 (1970)
Homar et al, IEEE JQE **32**, 553 (1996)
Javaloyes and Balle, IEEE JQE **45**, 431 (2009)

I.d. Objectives

- Study spatio-temporal dynamics in Ring Lasers.

- Construct a model that retains the spatial effects and the coupling between the different longitudinal modes ⟶ TWM

- Develop ONE tool to study different problems, e.g. Multi-mode behaviour, Different Optical Cavities, Directional Switching, Mode-locking...

II. Modal Structure of Ring Lasers

a. Modes of a Fabry-Pérot cavity
b. Ring Resonator with a Localized Imperfection
c. Modal Structure of a Semiconductor Ring Laser with Output Waveguides

S. Fürst, A. Pérez-Serrano, A. Scirè, M. Sorel and S. Balle,
Appl. Phys. Lett. 93, 251109 (2008)

II.a. Modes of a Fabry-Pérot cavity

Electric field:

$$E(z,\omega) = A_F(\omega)e^{iq(\omega)z} + A_B(\omega)e^{-iq(\omega)z}$$

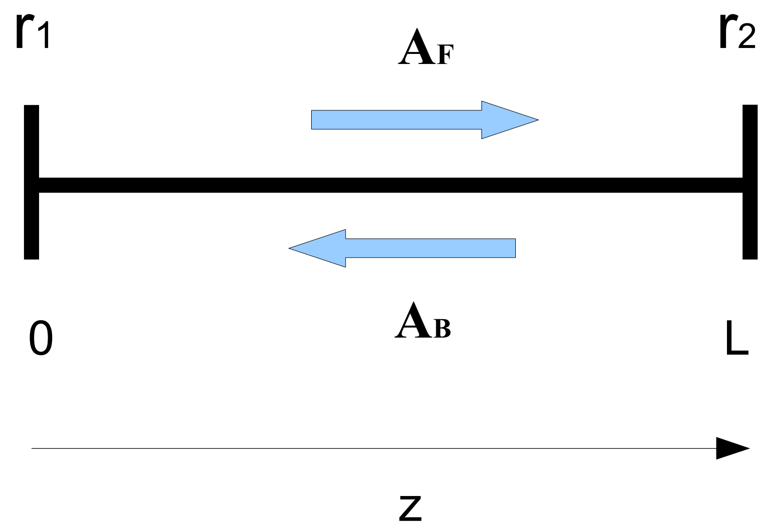

Boundary conditions:

$$\begin{cases} A_F = r_1 A_B \\ A_B e^{-iqL} = r_2 A_F e^{iqL} \end{cases}$$

Wave number:

$$\boxed{q = \frac{\pi m}{L} + \frac{i}{2L}\ln(r_1 r_2)}$$

$$m = 0, \pm 1, \pm 2, \ldots$$

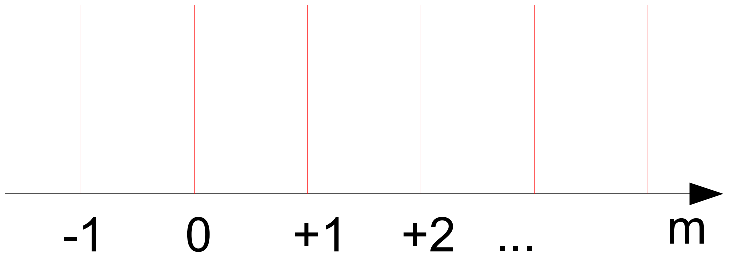

II.b. Ring resonator with a localized imperfection

Electric field:

$$E(z,\omega) = A_F(\omega)e^{iq(\omega)z} + A_B(\omega)e^{-iq(\omega)z}$$

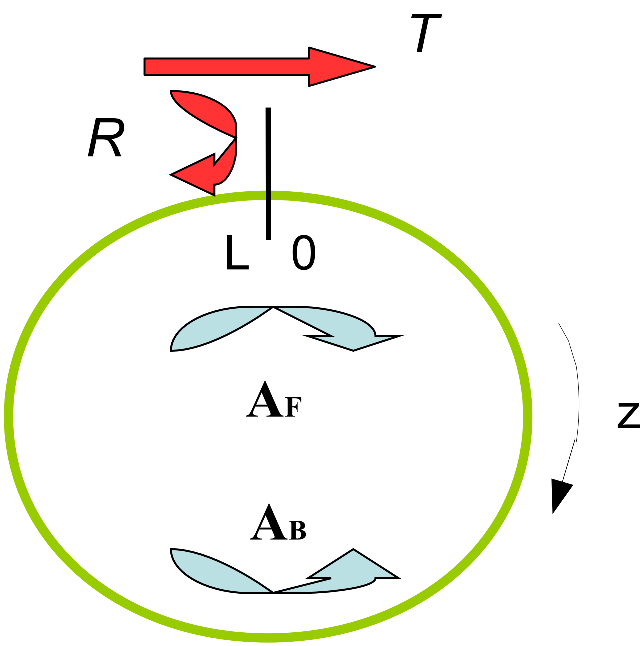

Boundary conditions:

$$\begin{cases} A_F = RA_B + TA_F e^{iq(\omega)L} \\ A_B e^{-iq(\omega)L} = RA_F e^{iq(\omega)L} + TA_B \end{cases}$$

Ideal ring ($R = 0$, $T = 1$) :

$$q = \frac{2\pi m}{L} \qquad m = 0, \pm 1, \pm 2, \ldots$$

General case ($R \neq 0$, $T \neq 0$) :

$$q_\pm = \frac{2\pi m}{L} + \frac{i}{L}\ln(T \pm R) \qquad m = 0, \pm 1, \pm 2, \ldots$$

Two families of solutions

II.b. Ring resonator with a localized imperfection

Conservation law and reciprocity conditions:

$$\begin{cases} |T|^2 + |R|^2 = 1 \\ RT^* + R^*T = 0 \end{cases} \rightarrow |T \pm R| = 1 \longrightarrow T \pm R = e^{i\theta_\pm}$$

$$\theta_\pm(R) = -\arctan\frac{\mathbb{I}m(R)}{\mathbb{R}e(R)} \pm \arcsin|R|$$

$$q_\pm(\omega) = \frac{2\pi m}{L} + \frac{\theta_\pm(R)}{L} \qquad m = 0, \pm 1, \pm 2, \ldots$$

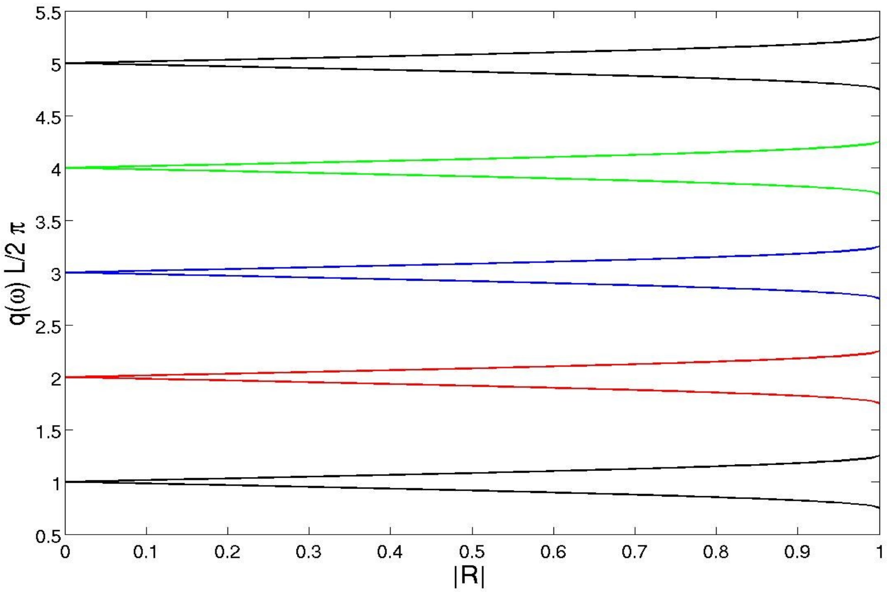

Splitting if $0 < |R| < 1$

Limits:

- $R = 1$ ⟶ Fabry-Pérot
- $R = 0$ ⟶ Ideal ring

II.c. Modal Structure of a Semiconductor Ring Laser with Output Waveguides

Experimental Setup:

Performed by Sandor Fürst at Glasgow University

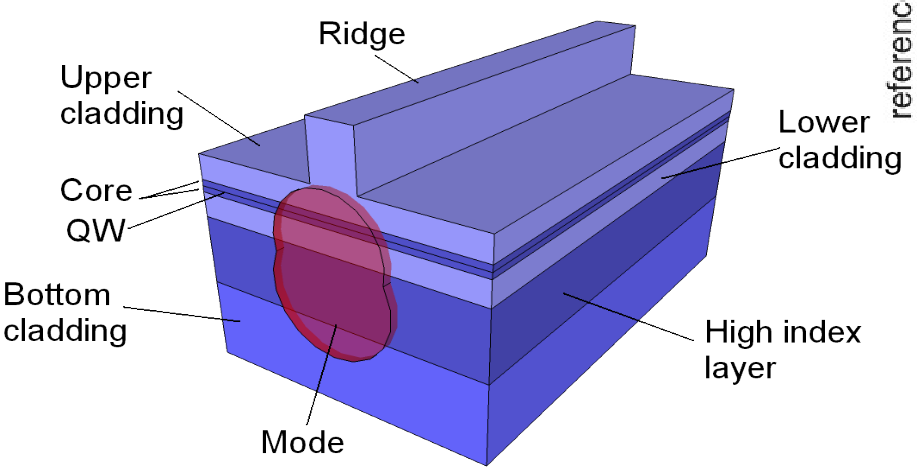

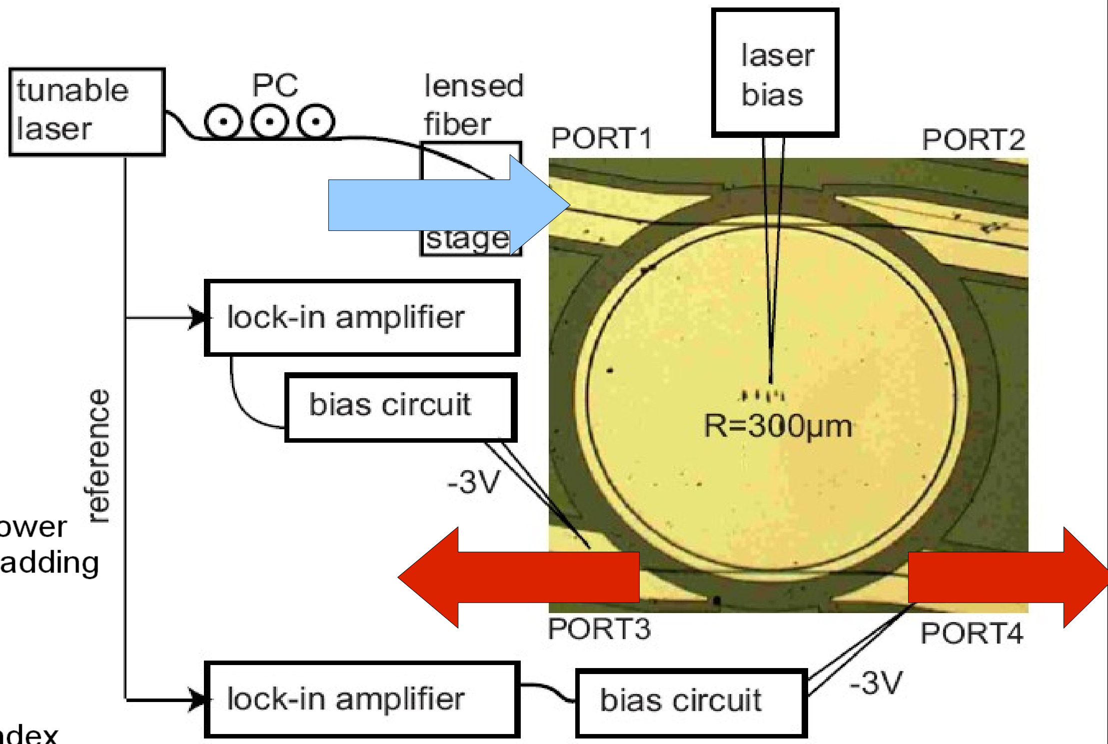

Courtesy of M.J. Strain (Glasgow Univ.)

II.c. Experimental Results

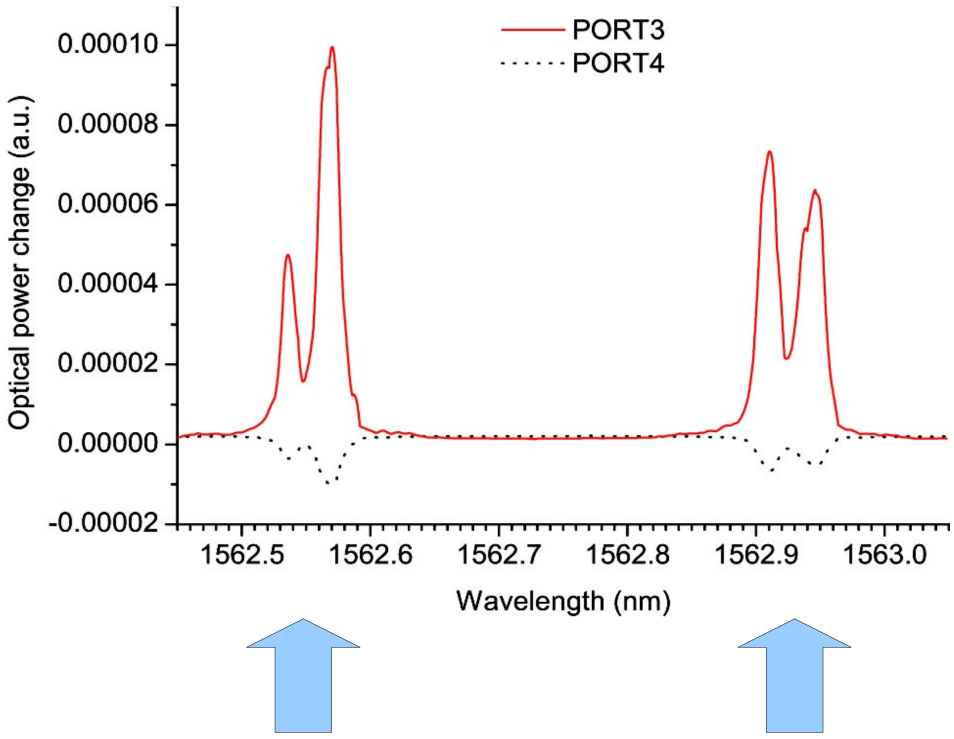

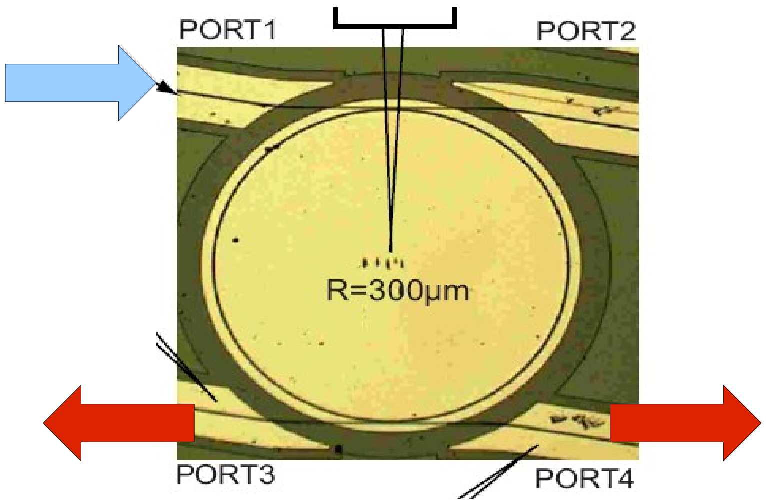

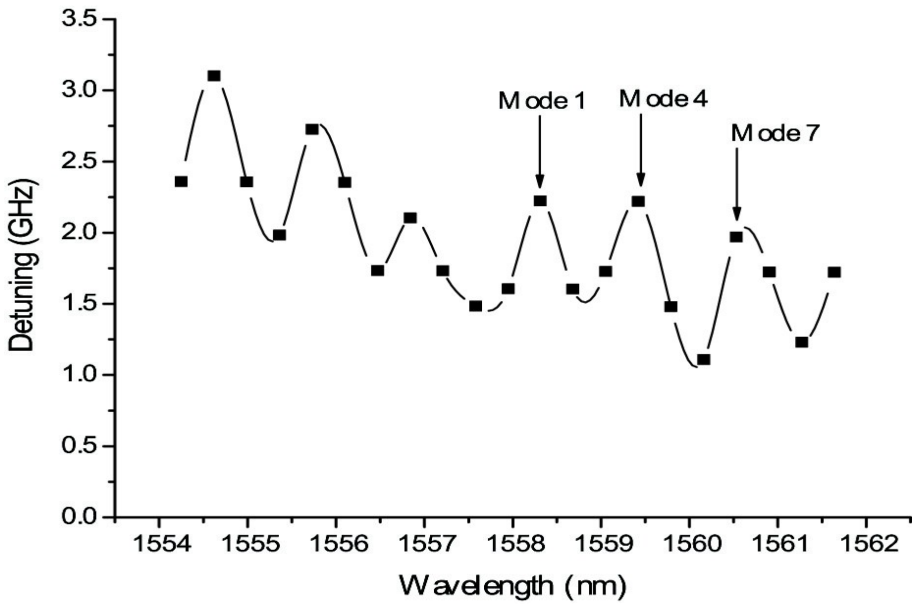

Ideal Ring Modes

II.c. Theoretical Analysis

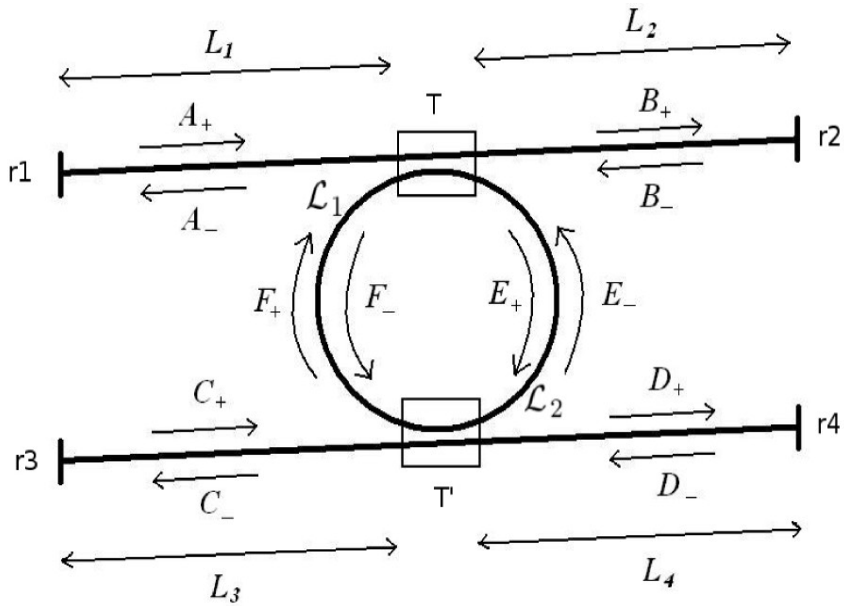

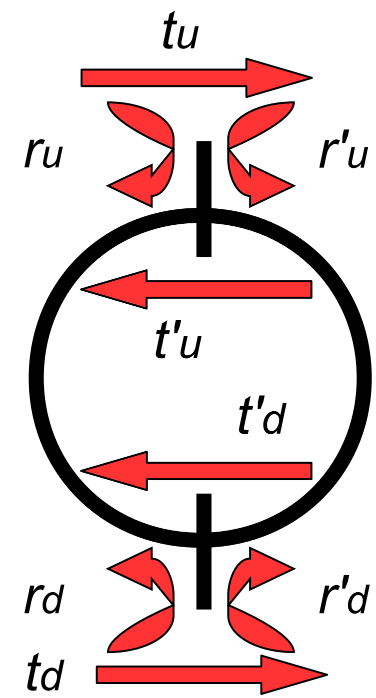

Round Trip Condition: $$e^{2iqL} - ae^{iqL} + b = 0$$

$$b = (r_u r'_u - t_u t'_u)^{-1} (r_d r'_d - t_d t'_d)^{-1}$$

$$a = (r_u r_d + r'_u r'_d + t'_u t_d + t_u t'_d) b$$

II.c. Theoretical Results

Modes: $$\boxed{q_m^{\pm} L = 2\pi m - i \ln Q_{\pm}}$$ $$Q_{\pm} = a/2 \pm [(a/2)^2 - b]^{1/2}$$

Experimental

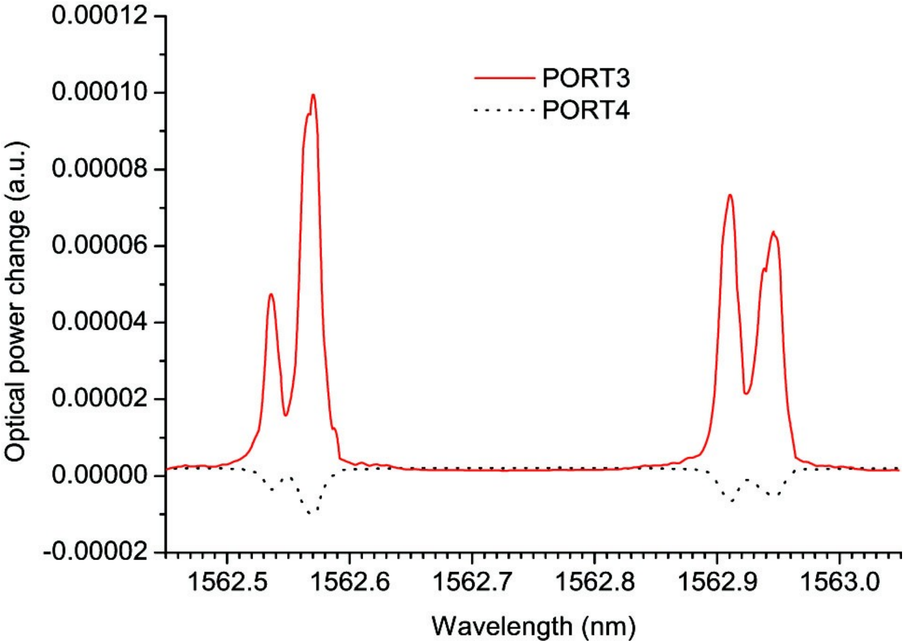

Theoretical

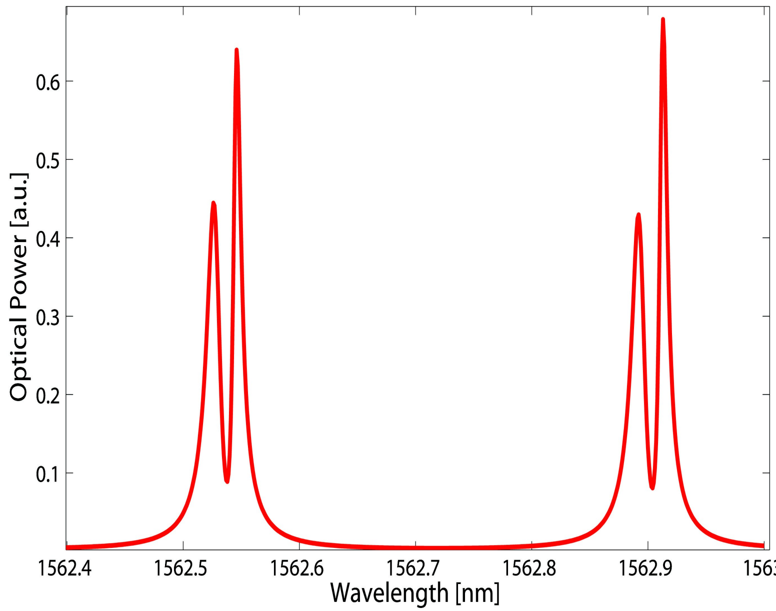

II.c. Theoretical Results

Experimental

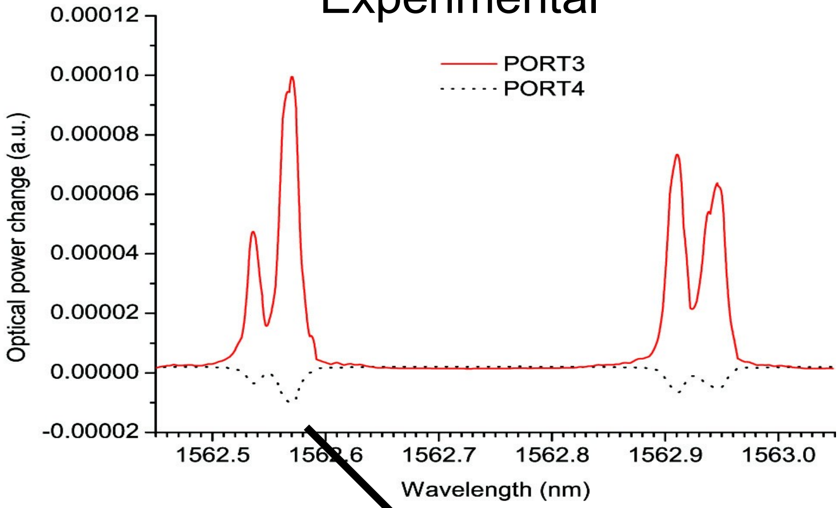

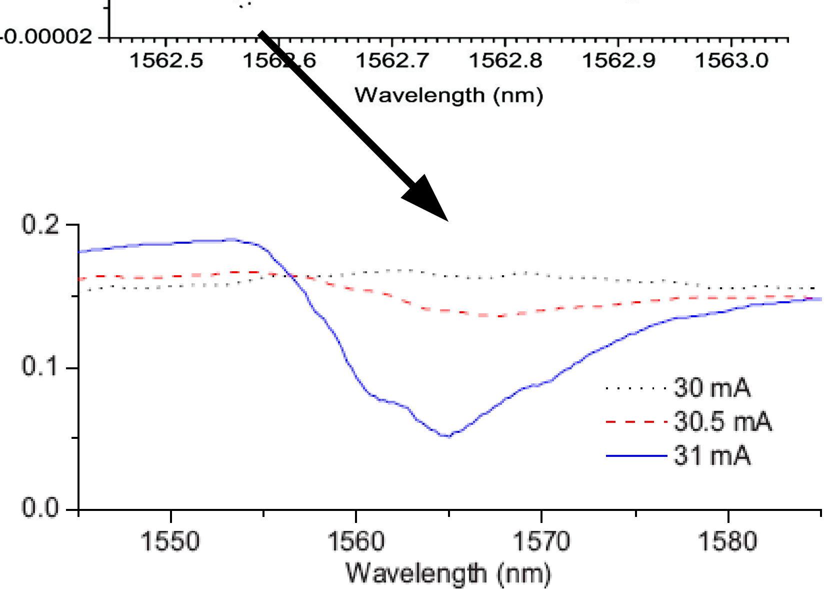

Theoretical

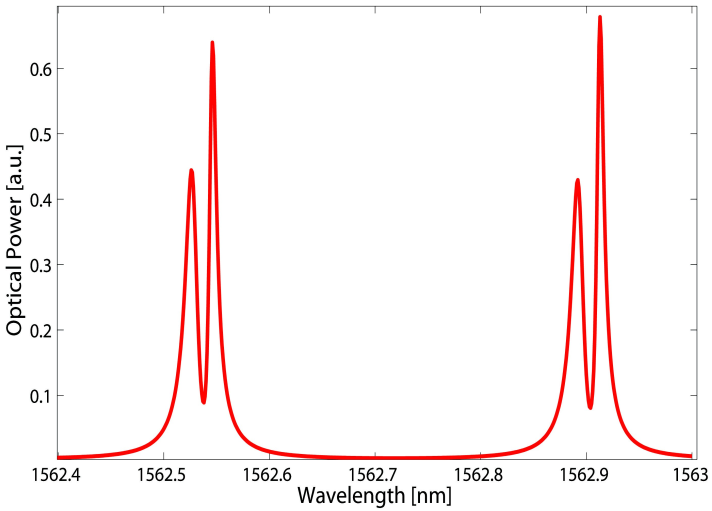

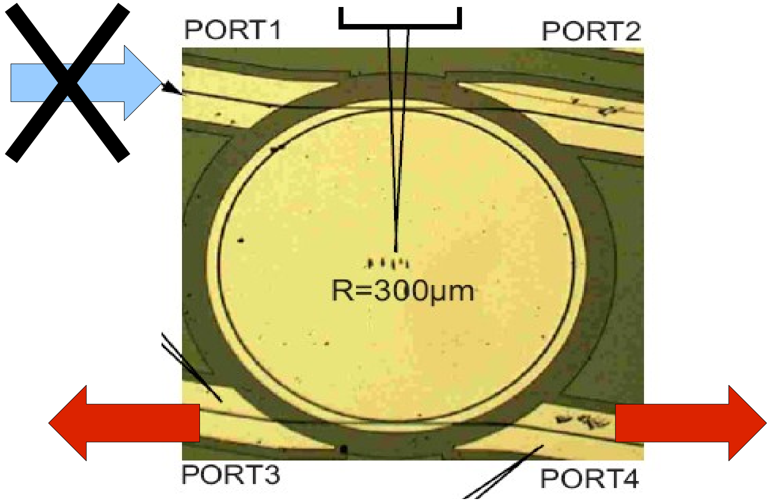

II.c. Theoretical Results

Experimental

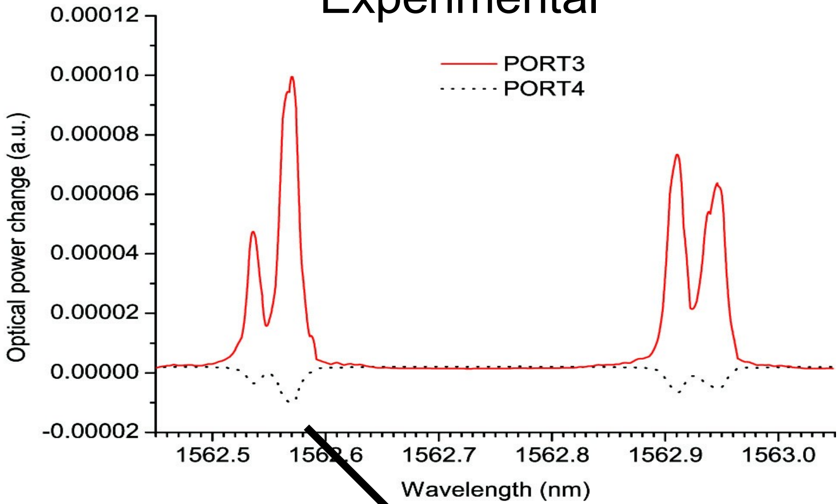

Theoretical

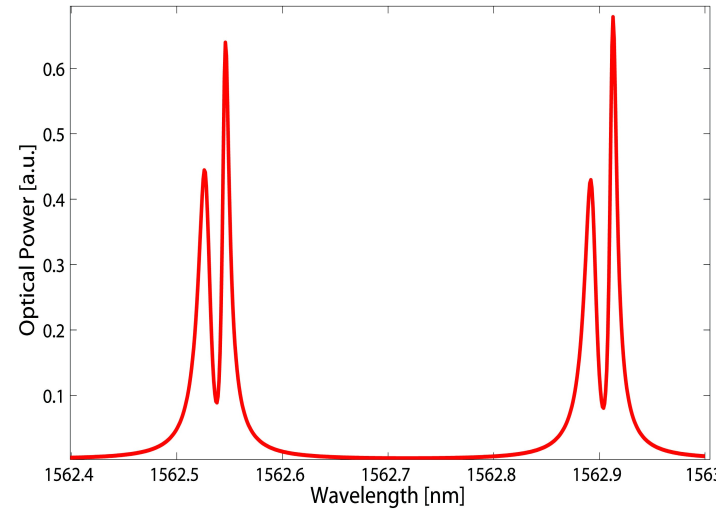

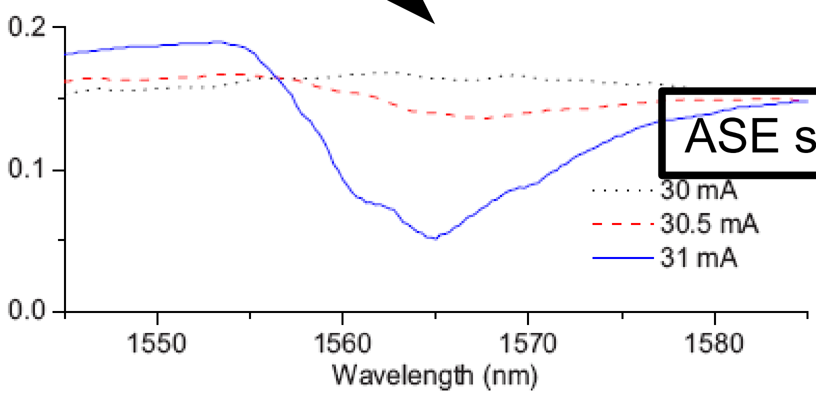

ASE suppression

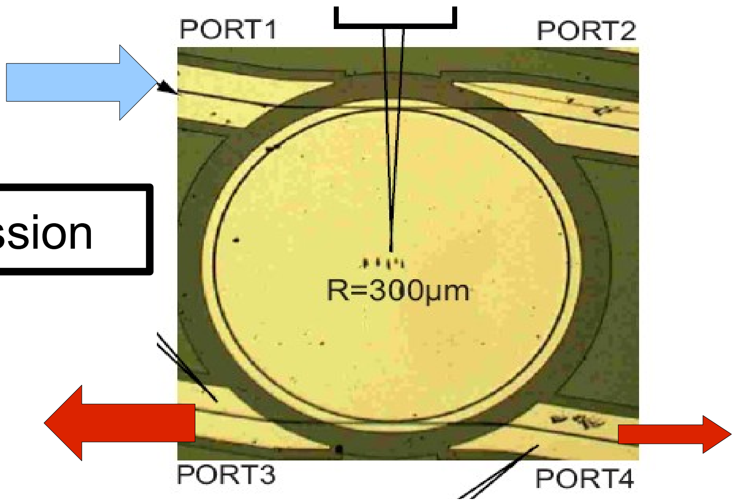

II.c. Theoretical Results

Splitting: $$\Delta = \frac{1}{2\pi}\left\{ \mathrm{Im}\left[\ln\left(\frac{Q_-}{Q_+}\right)\right] - \alpha\,\mathrm{Re}\left[\ln\left(\frac{Q_-}{Q_+}\right)\right]\right\}$$

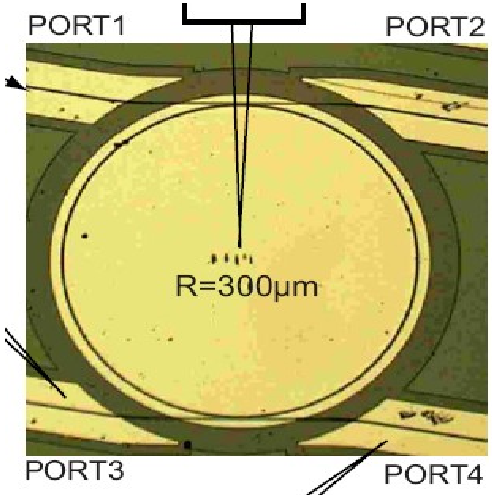

Experimental

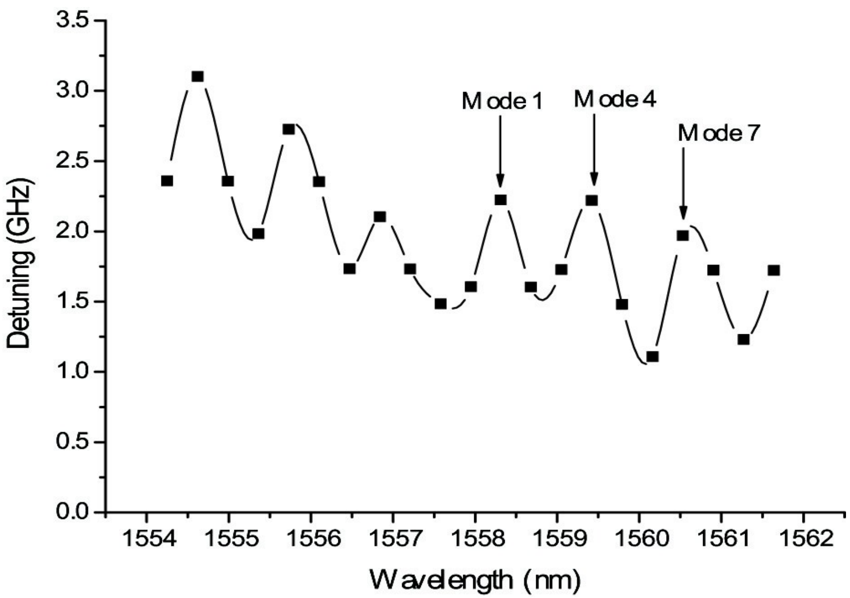

Theoretical

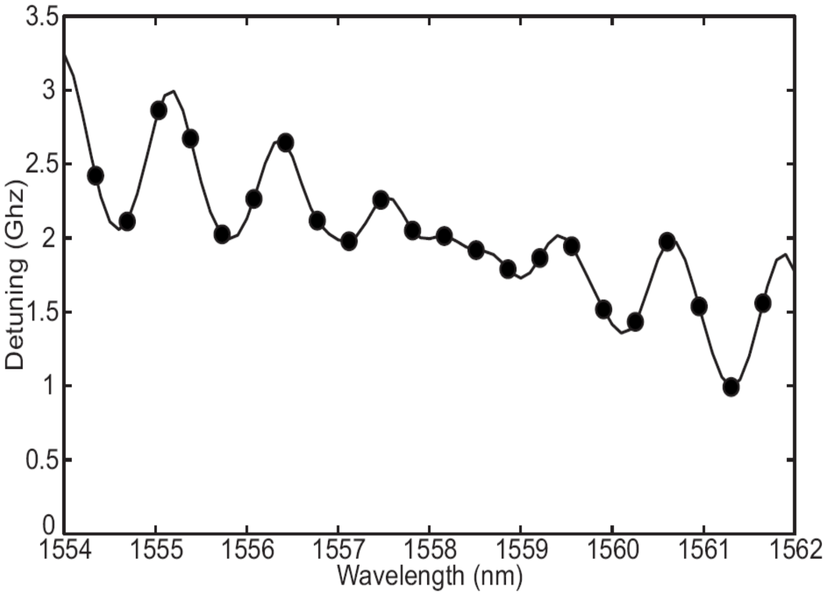

II. Conclusions

- We have experimentally studied the modal structure of SRLs by measuring the transfer function properties of the device biased close to the threshold.

- The residual reflectivities in the light-extraction sections determine the frequency splitting between two branches of solutions.

- These cavity effects determine the “cold” cavity properties of RLs, and possibly affect the dynamics of these systems.

III. Multimode Dynamics in Ring Lasers

a. The Model
b. Analytical Results and Test
c. Multimode Dynamics: Moderate Gain Bandwidth
d. Multimode Dynamics: Large Gain Bandwidth

A. Pérez-Serrano,J. Javaloyes and S. Balle,
Submitted to Phys. Rev. A

e. Other Geometries

M. Strain, A. Pérez-Serrano, A. Scirè, G. Verschaffelt,
J. Danckaert, M. Sorel and S. Balle, in preparation

III.a. The Model

Ingredients:

- Semi-classical approach

- Slowly varying amplitude approximation

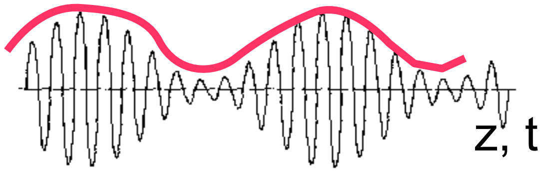

- Medium : 2 level atom

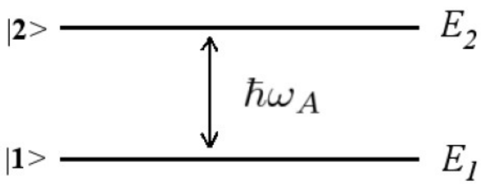

Narducci & Abraham, *Laser Physics and Lasers Instabilities*, World Scientific (1988)
Yariv, *Quantum Electronics*, Wiley (1989)

- Population Difference Grating induced by the counterpropagating fields (correction to the first order)

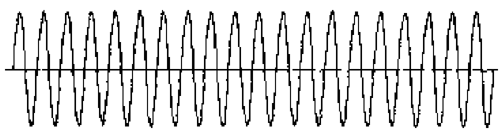

- Spontaneous Emission ⟶ $\xi_{\pm}(s,\tau)$

$$< \xi_{\pm}(s,\tau)\xi_{\pm}(s',\tau') >= \delta(\tau-\tau')\delta(s-s')$$

Homar et al, IEEE JQE **32**, 553 (1996)
Javaloyes and Balle, IEEE JQE **45**, 431 (2009)

III.a. The Model

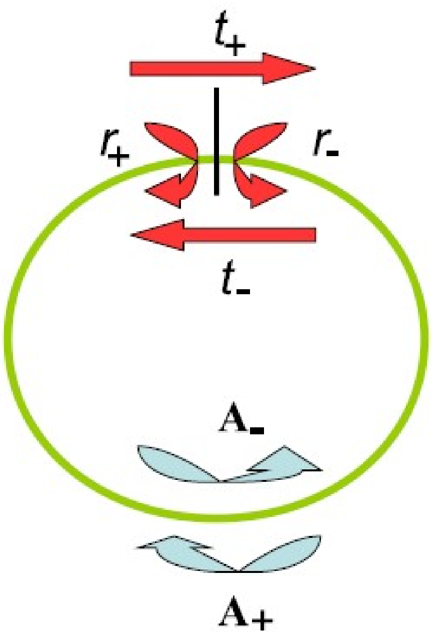

Dimensionless TW Equations:

$$\pm\frac{\partial A_\pm}{\partial s}+\frac{\partial A_\pm}{\partial \tau}=B_\pm-\alpha A_\pm$$

Electric Fields

Polarization

$$\frac{1}{\gamma}\frac{\partial B_\pm}{\partial \tau}=-(1+i\widetilde{\delta})B_\pm+g(D_0A_\pm+D_{\pm2}A_\mp)\;+\;\sqrt{\beta D_0}\,\xi_\pm(s,\tau)$$

$$\frac{\partial D_0}{\partial \tau}=\epsilon[J-D_0+\Delta\frac{\partial^2 D_0}{\partial s^2}-(A_+B_+^*+A_-B_-^*+A_+^*B_++A_-^*B_-)]$$

$$\frac{\partial D_{\pm2}}{\partial \tau}=-\eta D_{\pm2}-\epsilon(A_\pm B_\mp^*+A_\mp^*B_\pm)$$

Pop. diff.

Boundary Conditions:

$$\begin{aligned}A_+(0)&=t_+A_+(1)e^{i\gamma\widetilde{\omega}_0}+r_-A_-(0)\\A_-(1)e^{-i\gamma\widetilde{\omega}_0}&=t_-A_-(0)+r_+A_+(1)e^{i\gamma\widetilde{\omega}_0}\end{aligned}$$

III.a. The Model

Detuning:

$$\tilde{\delta} = \frac{\omega_A - \omega_0}{\gamma_\perp} = \tilde{\omega}_A - \tilde{\omega}_0$$

$$\gamma = \frac{\gamma_\perp n L}{c}$$

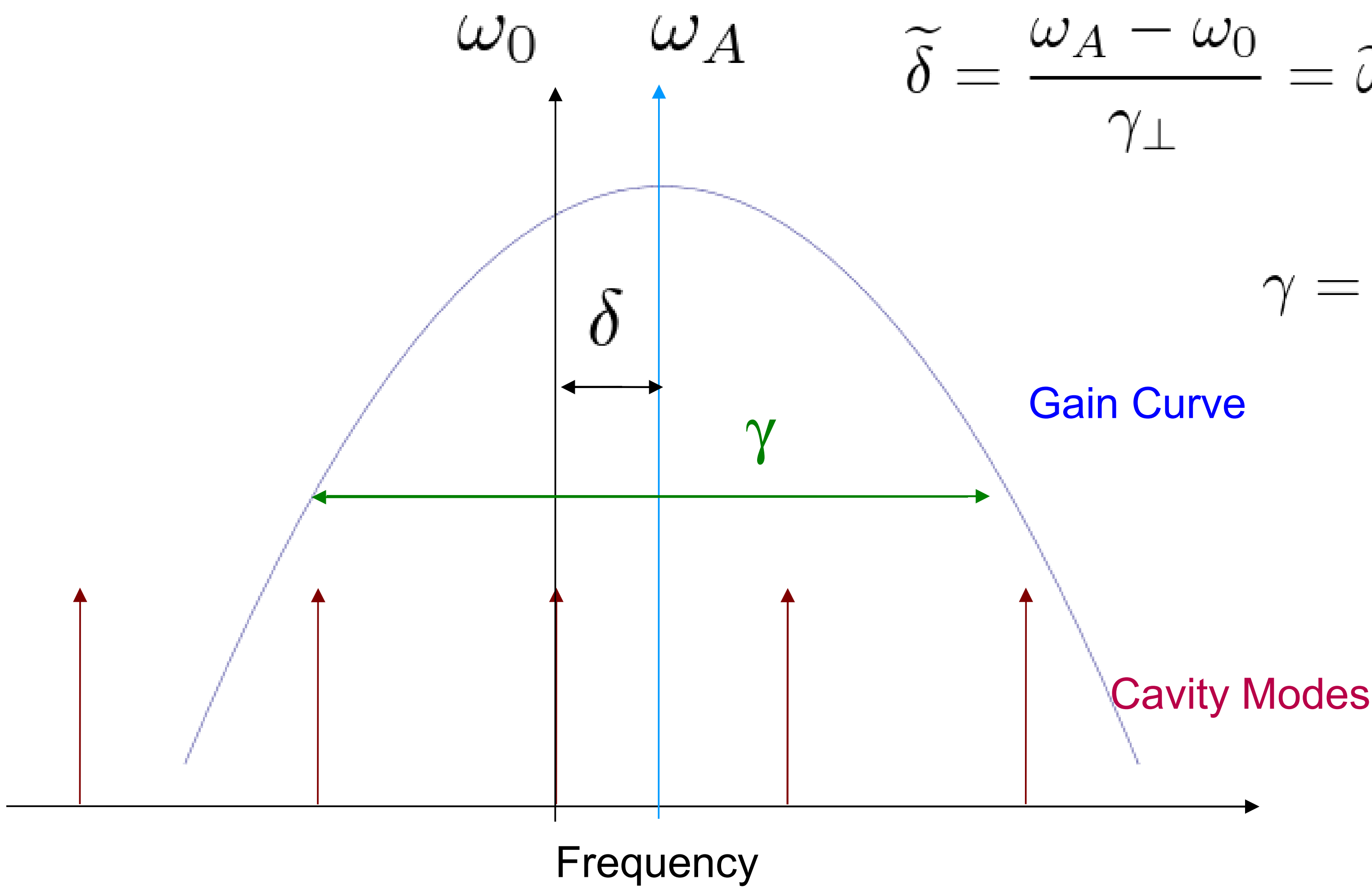

III.b. Analytical Results

Laser Threshold (LSA of the Off solution)

$$J_m^{th}(\sigma) = \frac{(\gamma\tilde{\delta} - 2\pi m)^2(\alpha - \ln(t + \sigma r))}{g(\alpha + \gamma - \ln(t+\sigma r))^2} - \frac{1}{g}\ln(t+\sigma r)$$

$$m = 0, \pm 1, \pm 2, \ldots$$

$$\sigma = \pm 1$$

Frequencies at Threshold

$$\Omega_m(\sigma) = \frac{2\pi m + \tilde{\delta}(\alpha - \ln(t+\sigma r))}{1 + \frac{1}{\gamma}(\alpha - \ln(t+\sigma r))}$$

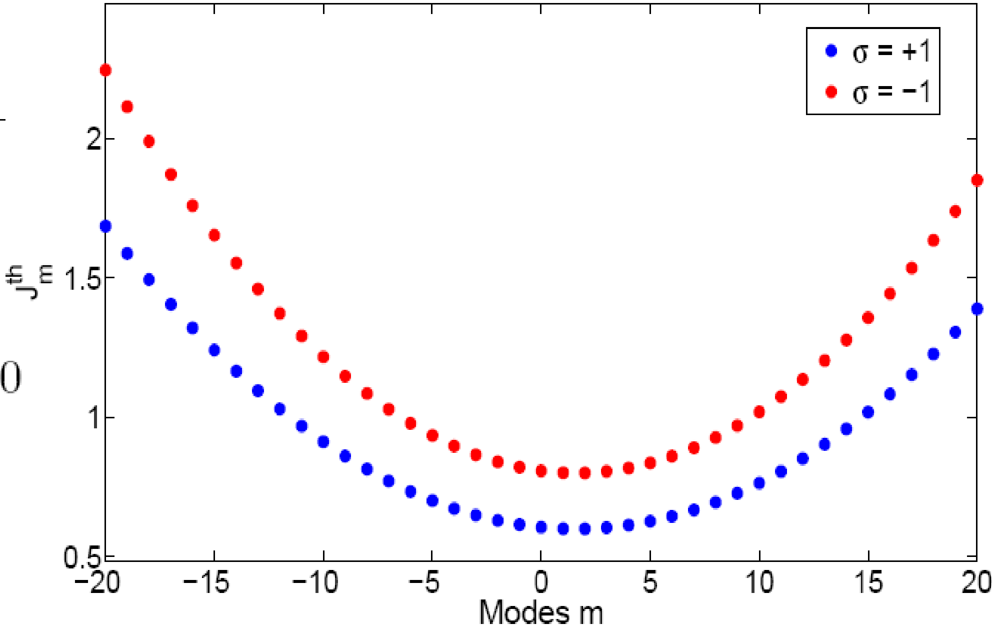

$$\tilde{\delta} = 0.1,\ g = 1,\ t = 0.5,\ r = 0.05,\ \alpha = 0$$
$$\gamma = 100$$

Lowest Threshold:
m = 2, J = 0.5981, $\sigma = +1$

III.b. Test: Single Mode Dynamics

$J = 0.5$ Fixed , scanning detuning

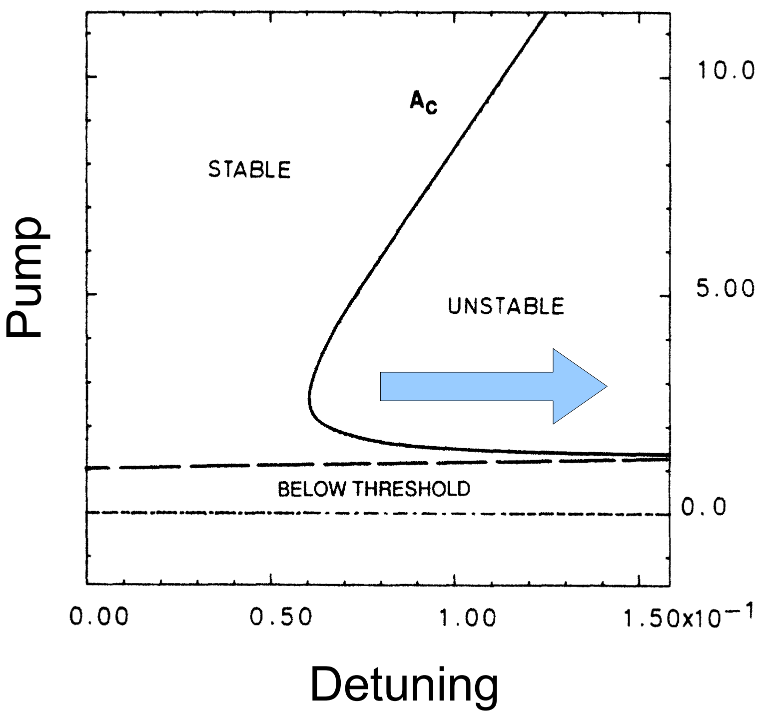

Zeghlache et al. PRA **37**, 470 (1988)

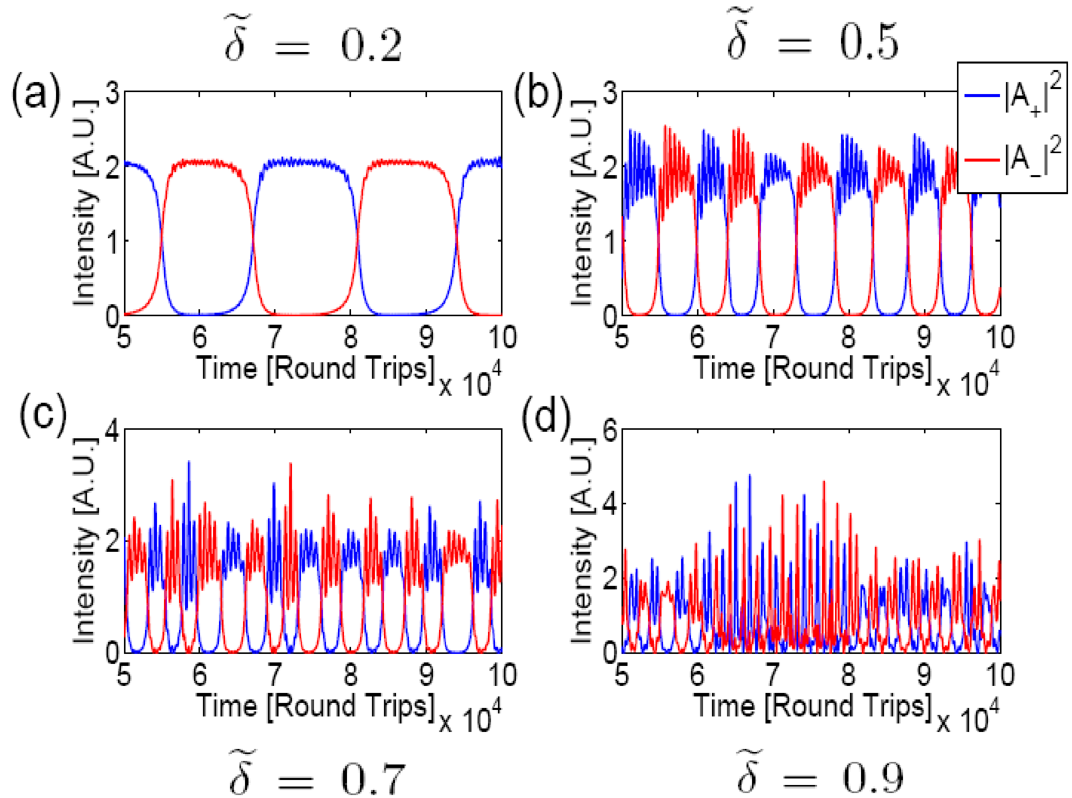

$g = 1,\ \epsilon = \eta = 1.78\ 10^{-5},\ \beta = 10^{-4},\ t = 0.9,\ r = 0,\ \alpha = 0$

$\gamma = 1$ Mesh points $N = 100$

III.b. Test: Single Mode Dynamics

$\tilde{\delta} = 0.2$ Fixed, scanning Pump

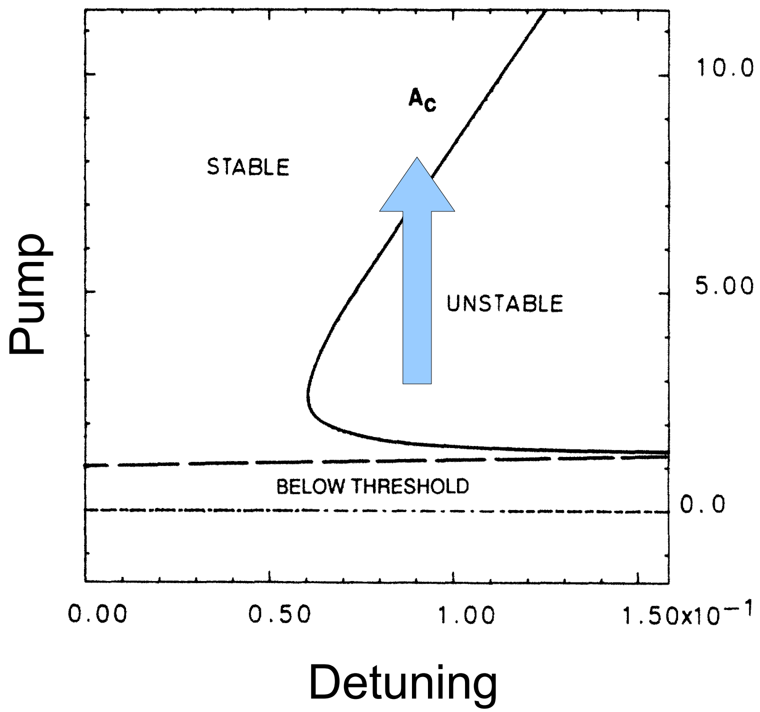

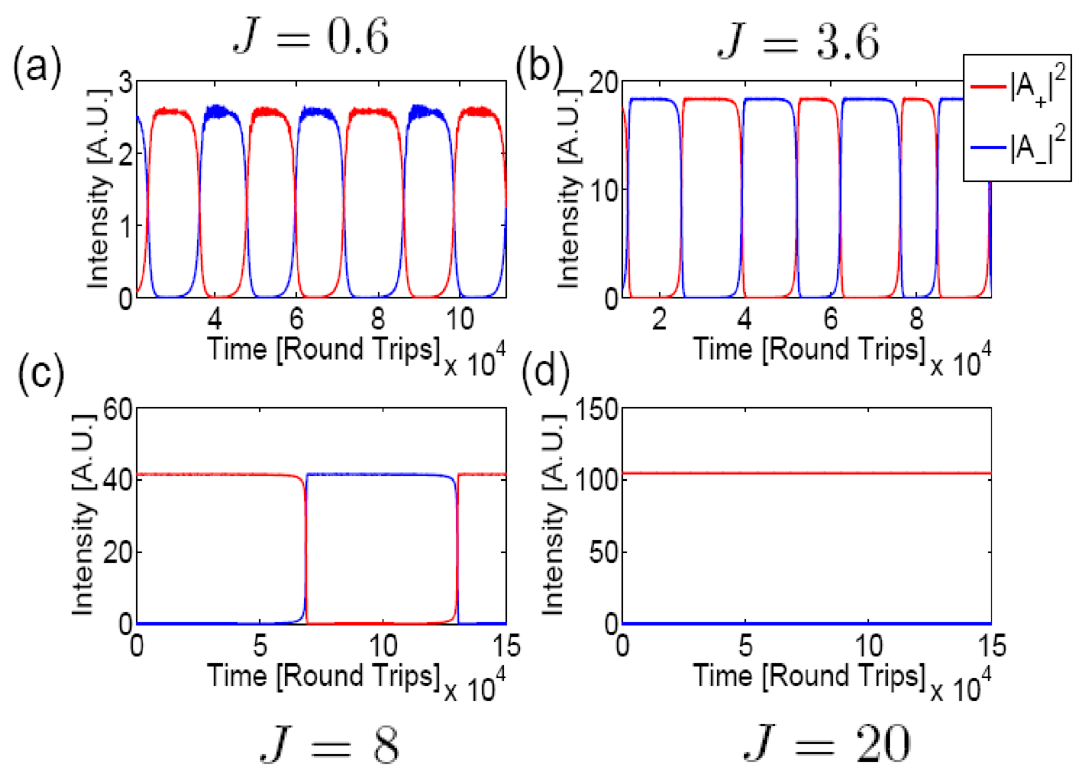

$$g = 1,\ \epsilon = \eta = 1.78\ 10^{-5},\ \beta = 10^{-4},\ t = 0.9,\ r = 0,\ \alpha = 0$$

$$\gamma = 1 \qquad \text{Mesh points } N = 100$$

Zeghlache et al. PRA **37**, 470 (1988)

III.c. Multimode Dynamics

Dependence on:

Detuning (δ)

Gain curve bandwidth (γ)

$$|\tilde{\delta}| \leq \frac{\pi}{\gamma}$$

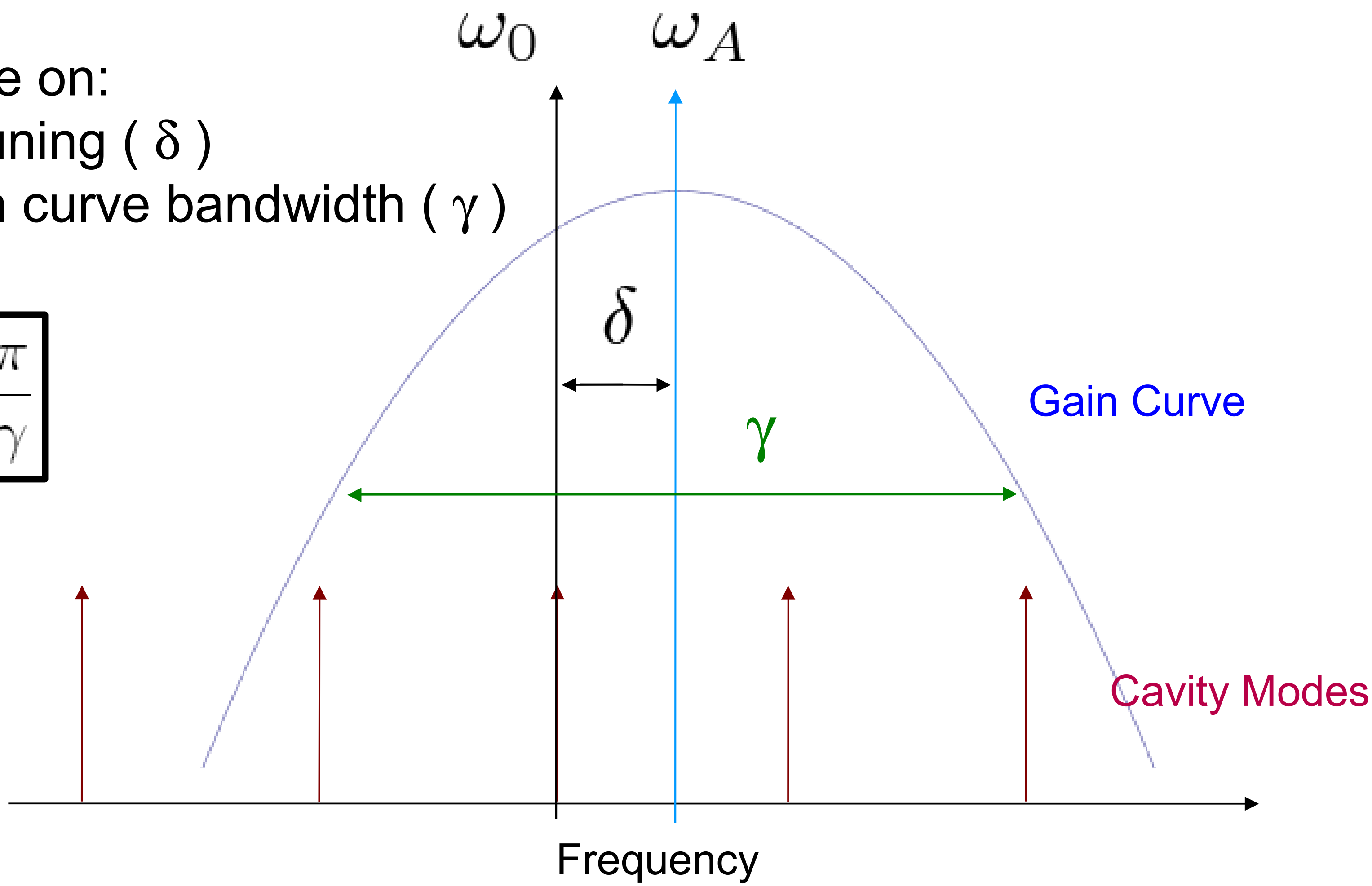

III.c. Multimode Dynamics: Moderate Gain bandwidth

$\widetilde{\delta} = 0.3141$

$\gamma = 10$

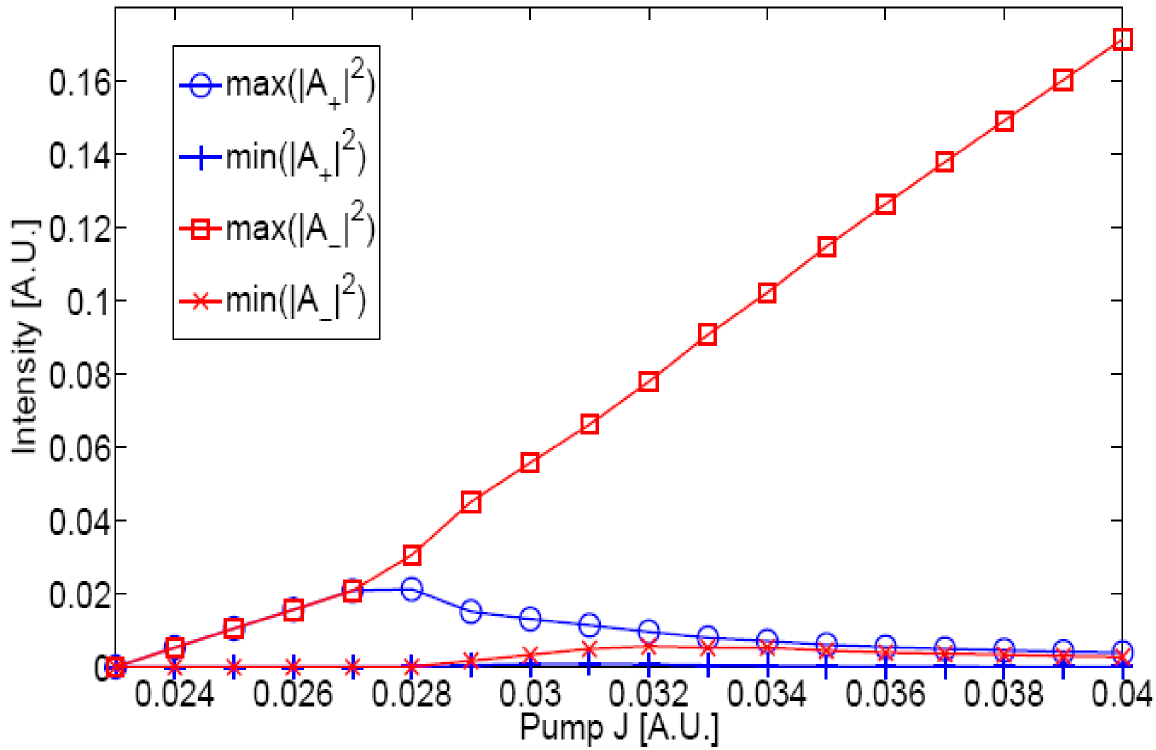

Mesh points $N = 100$, $\widetilde{\delta} = 0.3141$, $g = 5$, $\epsilon = 10^{-2}$, $\eta = 0.1$, $\beta = 10^{-4}$, $t = 0.9$, $r = 5\ 10^{-4}$, $\alpha = 0$

III.c. Multimode Dynamics: Moderate Gain bandwidth

Multistability !

$\widetilde{\delta} = 0.3141$

$\gamma = 10$

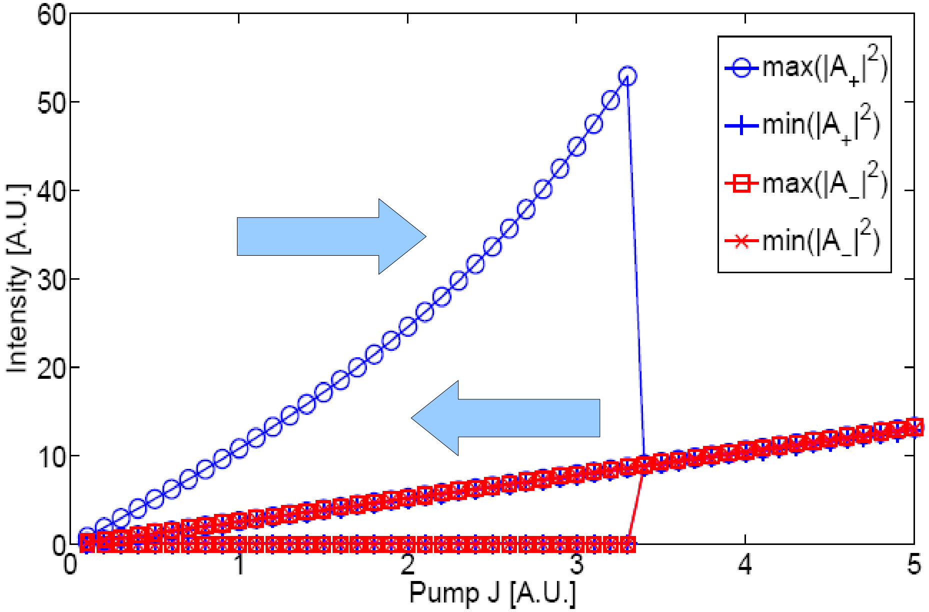

$\mathrm{Mesh\ points}\ N = 100,\ \widetilde{\delta} = 0.3141,\ g = 5,\ \epsilon = 10^{-2},$
$\eta = 0.1,\ \beta = 10^{-4},\ t = 0.9,\ r = 5\ 10^{-4},\ \alpha = 0$

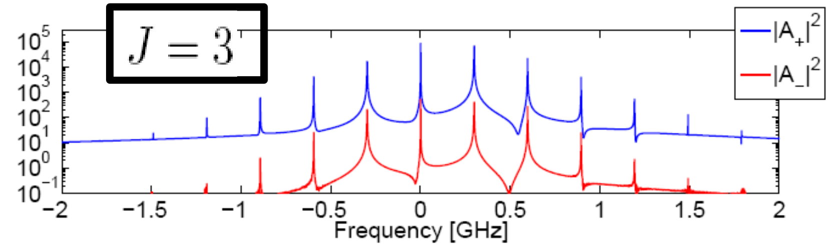

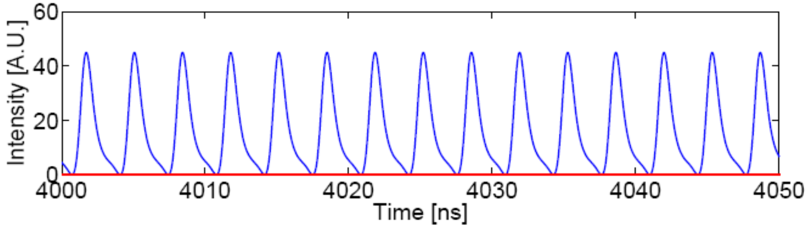

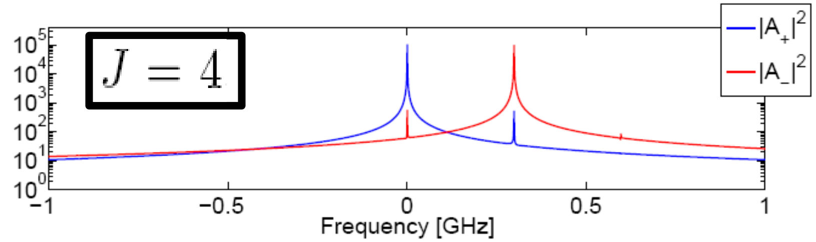

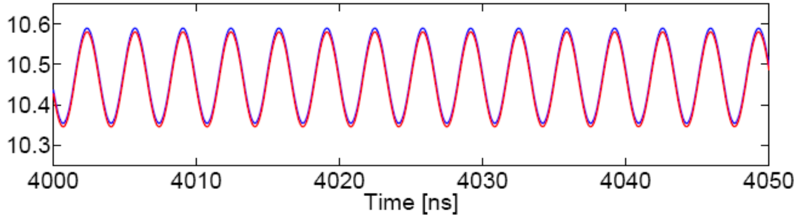

IFISC

III.c. Multimode Dynamics: Moderate Gain bandwidth

Multistability !

$\widetilde{\delta} = 0.3$

$\gamma = 10$

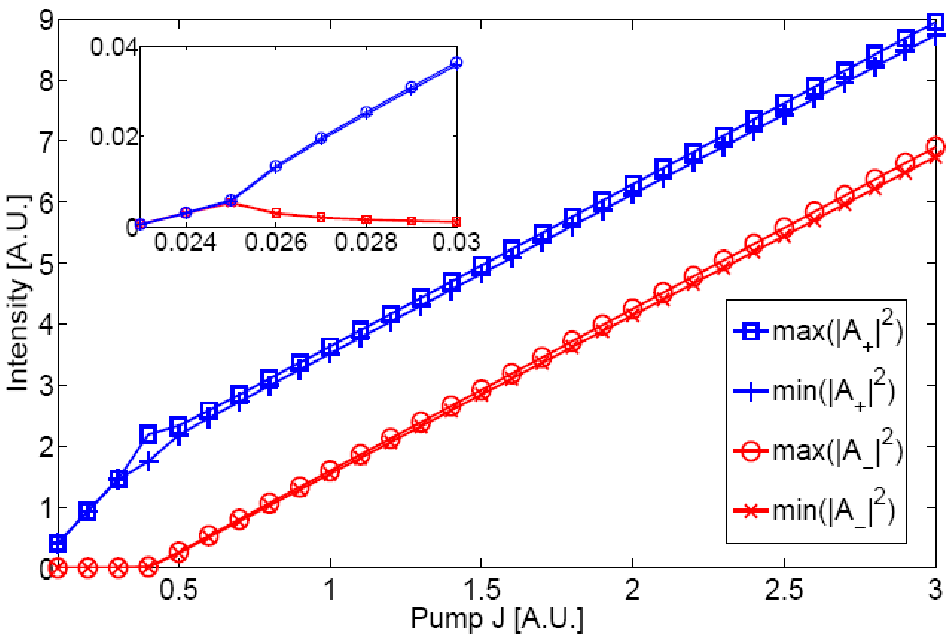

Mesh points $N = 400$, $g = 5$, $\epsilon = 10^{-2}$, $\eta = 0.1$, $\beta = 10^{-4}$, $t = 0.9$, $r = 5\ 10^{-4}$ $\alpha = 0$

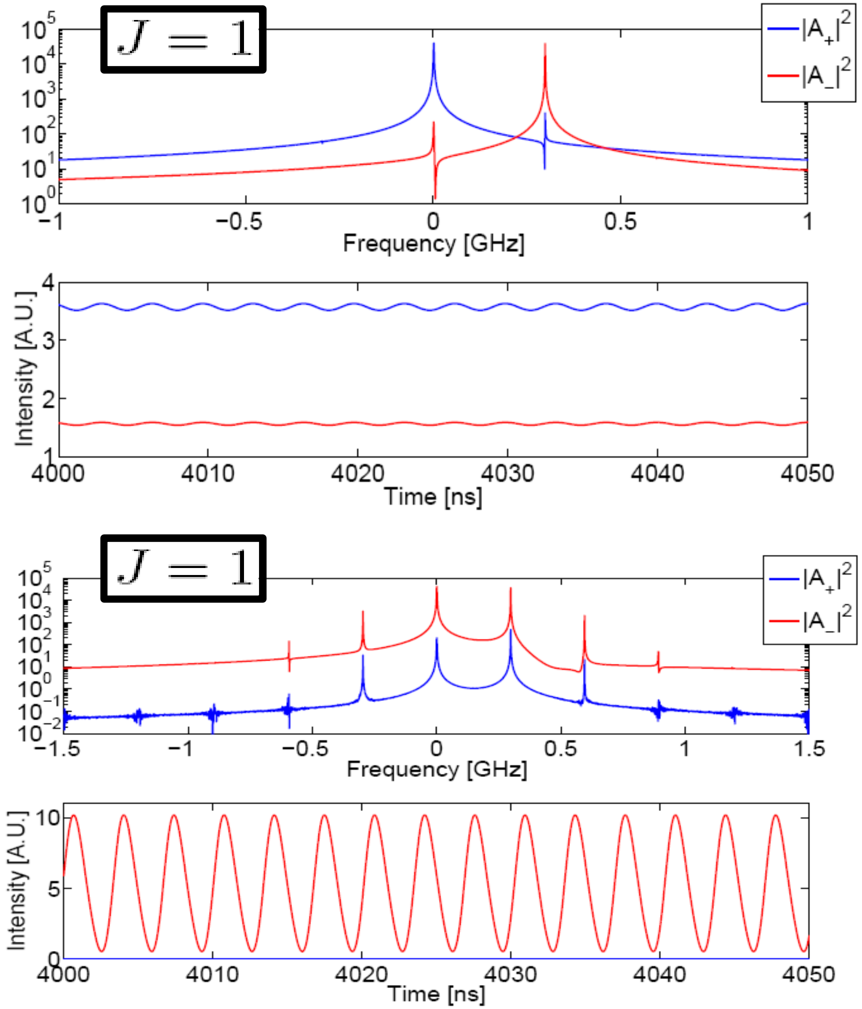

III.d. Multimode Dynamics: Large Gain bandwidth

$\gamma = 100$

$\tilde{\delta} = 0.03141$

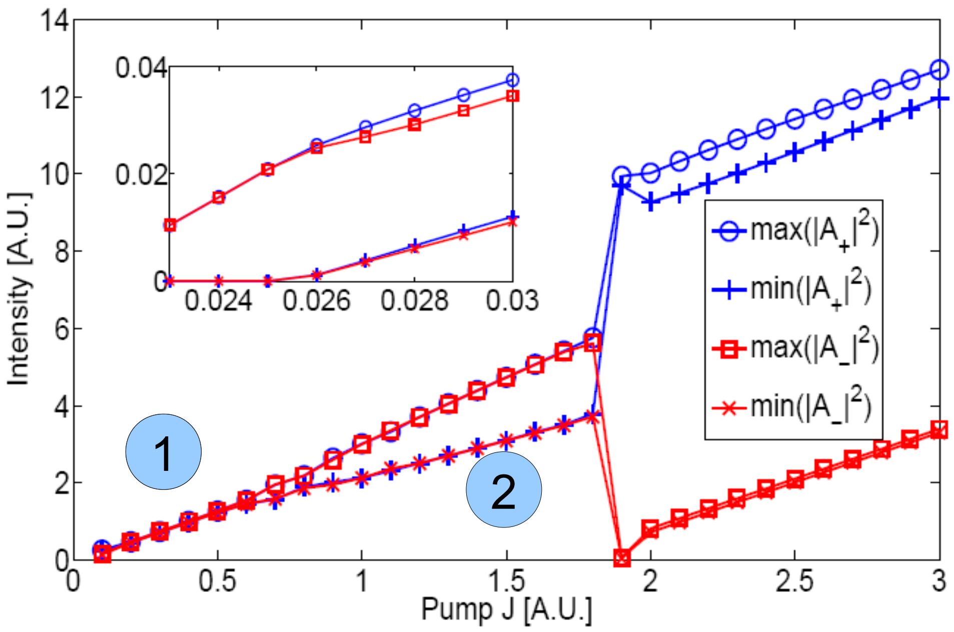

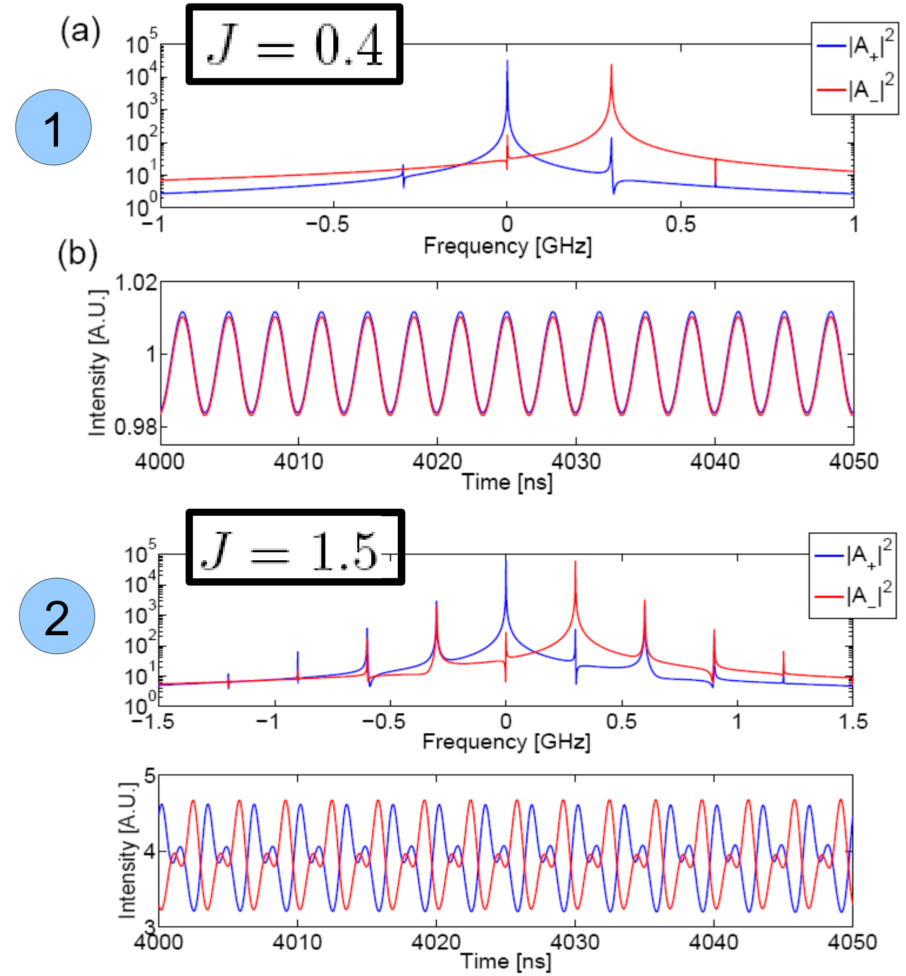

Mesh points $N = 400$, $g = 5$, $\epsilon = 10^{-2}$, $\eta = 2\ 10^{-2}$,
$\beta = 10^{-4}$, $t = 0.9$, $r = 5\ 10^{-4}$ $\quad \alpha = 0$

III.d. Multimode Dynamics: Large Gain bandwidth

$\gamma = 100$

$\tilde{\delta} = 0.03141$

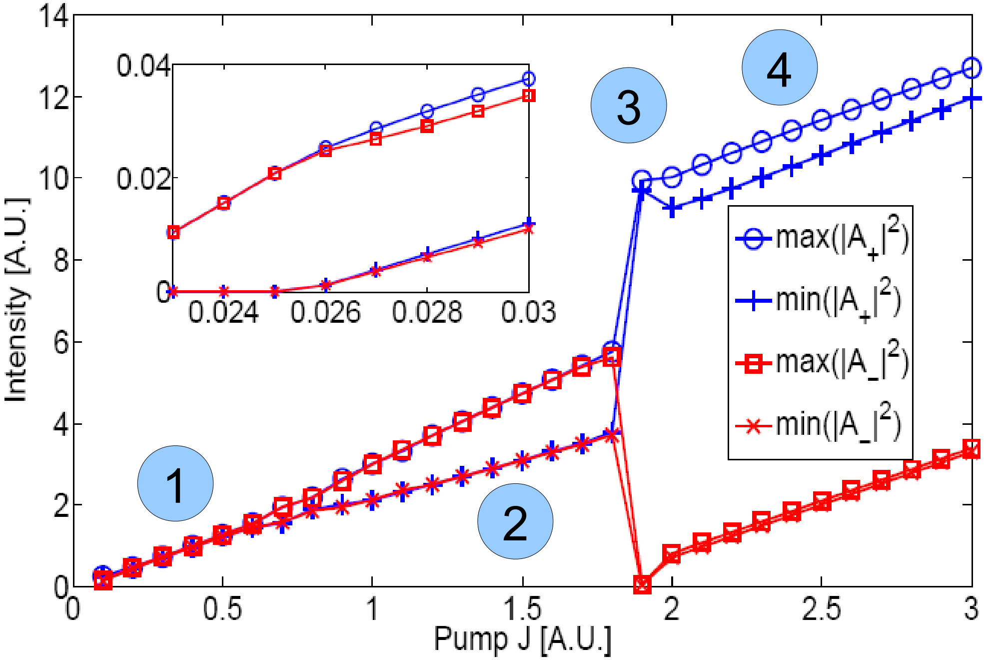

Mesh points $N = 400$, $g = 5$, $\epsilon = 10^{-2}$, $\eta = 2\ 10^{-2}$,
$\beta = 10^{-4}$, $t = 0.9$, $r = 5\ 10^{-4}$ $\alpha = 0$

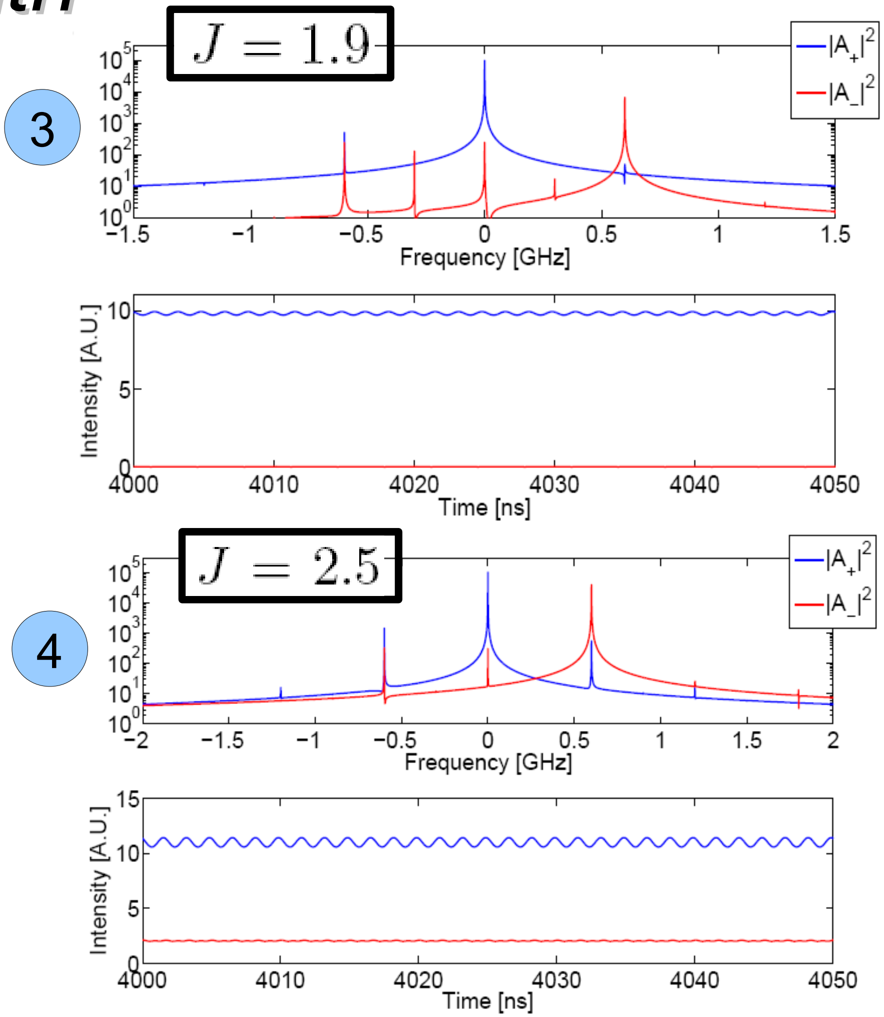

III.d. Multimode Dynamics: Large Gain bandwidth

$\gamma = 100$

$\tilde{\delta} = 0.015$

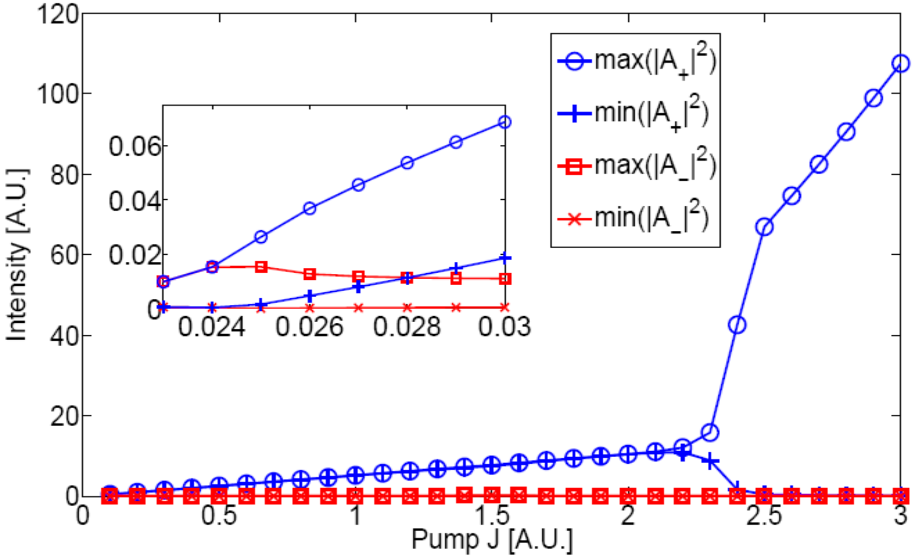

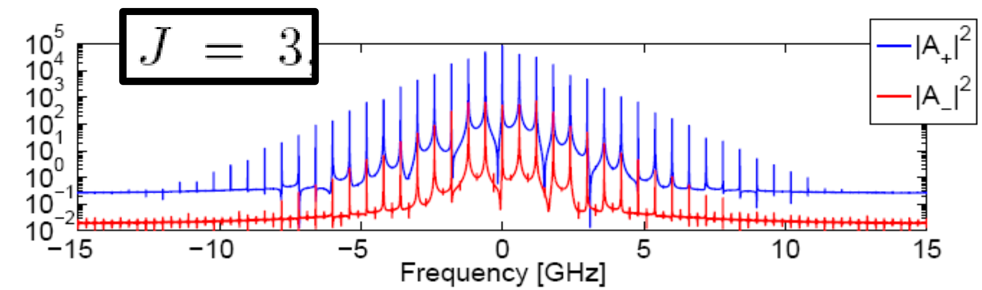

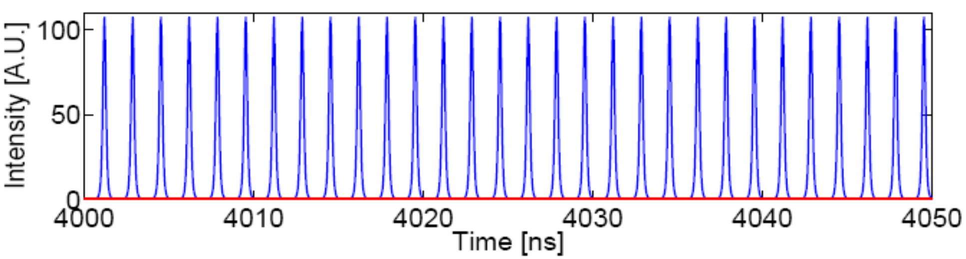

Mesh points $N = 400$, $g = 5$, $\epsilon = 10^{-2}$,
$\eta = 2\ 10^{-2}$, $\beta = 10^{-4}$, $t = 0.9$, $r = 5\ 10^{-4}$ $\alpha = 0$

III.e. Other Geometries

C++ (Object Oriented Language) → Discretized Elements

- WGuide (N points Wave Guide)

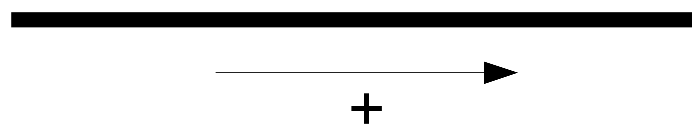

- PointTR
(Point Transimission and Reflection with losses)

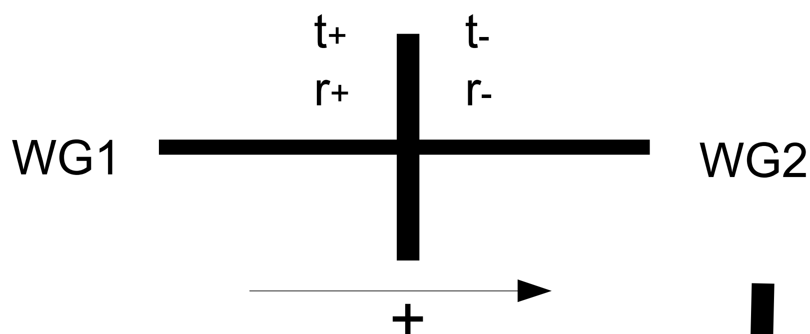

- PointC
(Point Coupler without losses)

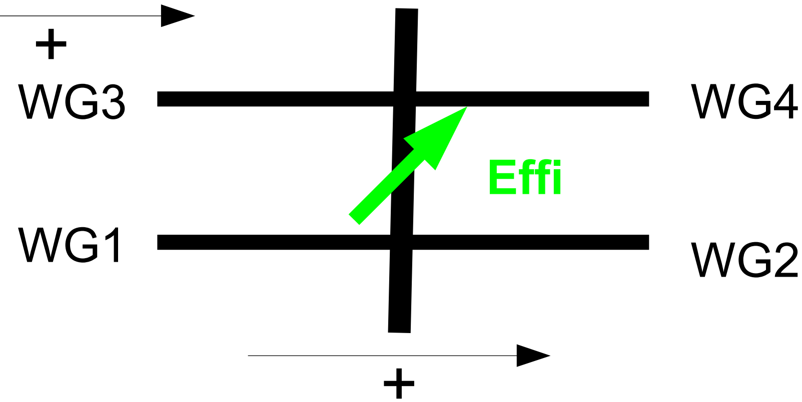

...

III.e. Other Geometries

In progress...

Fabry-Pérot:

Ring Laser:

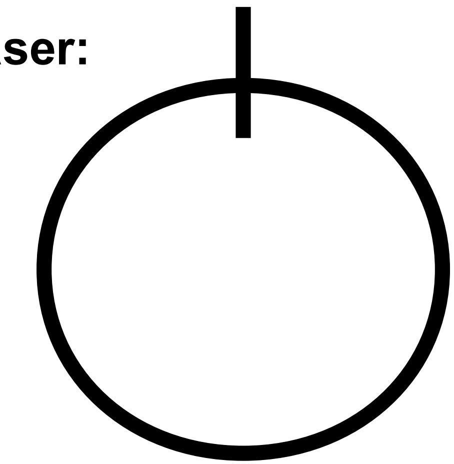

Ring Laser with Output Waveguides :

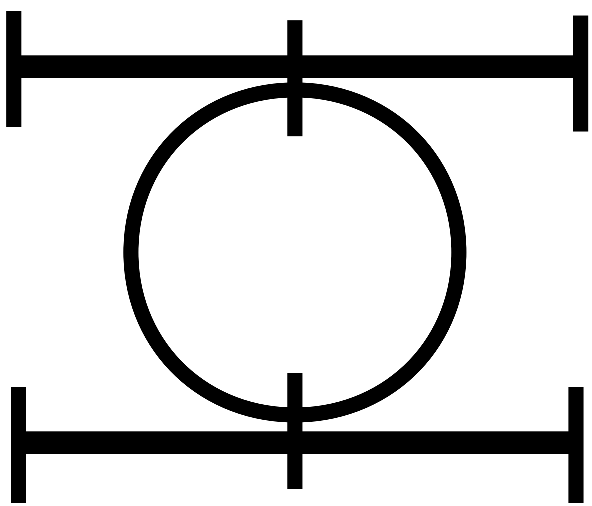

Coupled Rings:

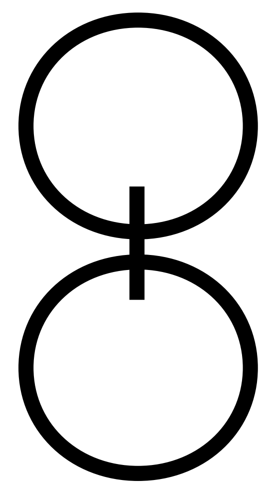

In progress...

III.e. Other Geometries: Snail Laser

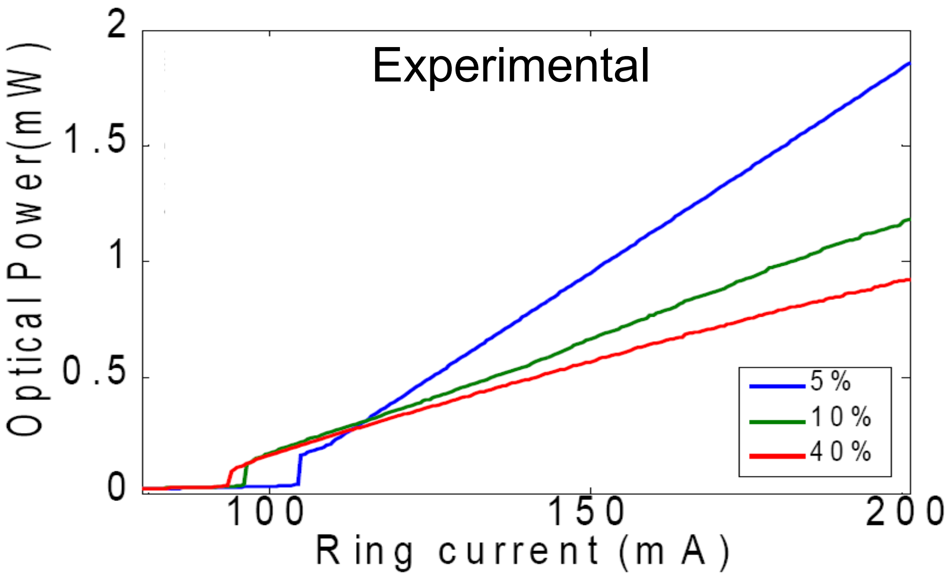

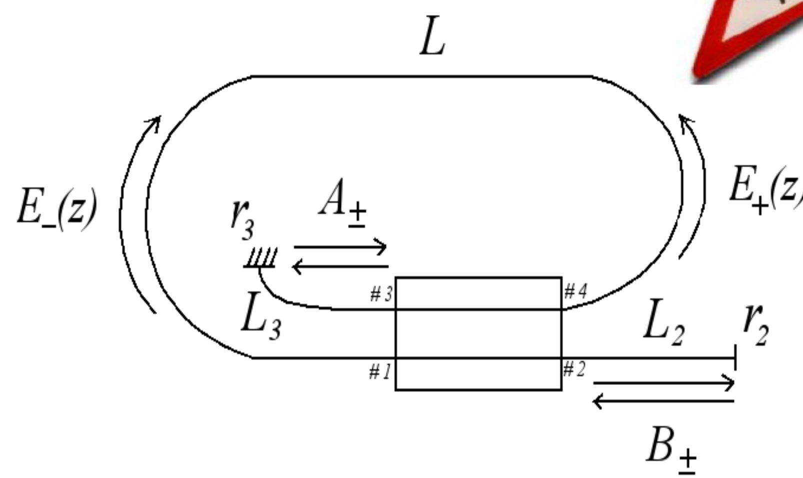

$$g = 1,\ \gamma = 10,\ \alpha = 1,\ \epsilon = 10^{-2},\ \eta = 10,$$
$$\tilde{\delta} = 0,\ r_2 = 0.2 \text{ and } r_3 = 0.6.$$

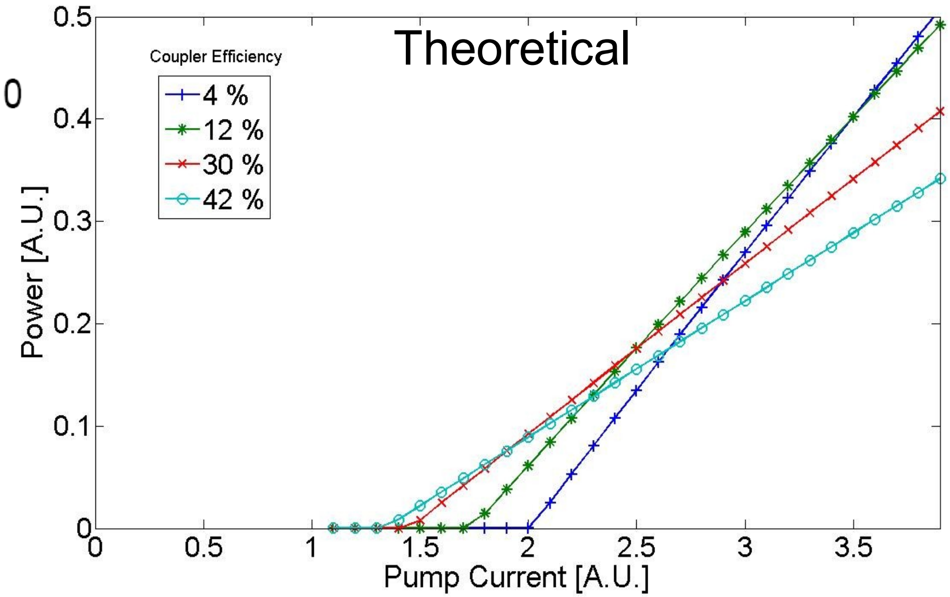

III. Conclusions

• The multimode dynamics of a two-level ring laser has been explored using a bidirectional TWM.

• The model and its numerical implementation have been tested by reproducing the dynamical results obtained in the singlemode limit.

• We have found novel dynamical regimes where the emission in each direction occurs at different wavelengths, each direction being associated to a different longitudinal mode.

• Mode-locked unidirectional emission is reported without introducing in the cavity any additional element that favors pulsed operation.

• We extended our model to simulate different laser cavities and coupled structures.

Thank you for your attention !

Acknowledgments:

Alessandro Scirè, Salvador Balle, Julien Javaloyes

Sandor Fürst, Michael J. Strain, Gabor Mezösi, Marc Sorel

Guy Verschaffelt, Jan Danckaert

www.iolos.org